Euclidean hub-and-spoke networks

John Gunnar Carlsson and Fan Jia*

June 20, 2013

Abstract

The hub-and-spoke distribution paradigm has been a fundamental principle in geographic network design for more than 40 years. One of the primary advantages that such networks possess is their ability to exploit economies of scale in transportation by aggregating network flows through common sources. In this paper, we consider the problem of designing an optimal hub-and-spoke network in continuous Euclidean space: the "spokes" of the network are distributed uniformly over a service region, and our objective is to determine the optimal number of hub nodes and their locations. We consider seven different backbone network topologies for connecting the hub nodes, namely the Steiner and minimum spanning trees, a travelling salesman tour, a star network, a capacitated vehicle routing tour, a complete bipartite graph, and a complete graph. We also perform an additional analysis on a multi-level network in which network flows move through multiple levels of transshipment before reaching the service region. We describe the asymptotically optimal (or near-optimal) configurations that minimize the total network costs as the demand in the region becomes large and give an approximation algorithm that solves our problem on a convex planar region for any values of the relevant input parameters.

1 Introduction

The hub-and-spoke distribution paradigm has been a fundamental principle in geographic network design for more than 40 years [15]. The distinguishing characteristic of such a network is that direct connections between locations in a geographic region are replaced with indirect connections facilitated with the use of hub nodes. As identified in [36], such a network topology is desirable because it reduces and simplifies network construction costs, centralizes commodity handling, and allows carriers to take advantage of economies of scale through consolidation of flows. It was noted in [14], for example, that for air traffic networks,

> The simplest manifestation of these economies of scale appear in areas such as maintenance, where staff and inventory costs can be reduced by having one central maintenance facility. A subtler and more important reason for hub-and-spoke arrangements, however, has to do with economies of scale applied to frequency and passenger preferences.... A hub-and-spoke network topology has a consolidating effect that makes it possible to justify more flights to each city.

Broadly speaking, the optimal size and shape of a hub-and-spoke network depends on costs from three sources:

1. *Fixed costs* incurred from installing, operating, and maintaining hub facilities,
2. *Backbone network costs* incurred from transporting goods along the network that connects the hubs, and
3. *Local transportation costs* incurred from transporting goods between hubs and spokes.

*Department of Industrial and Systems Engineering, University of Minnesota. J. G. C. gratefully acknowledges DARPA Young Faculty Award N66001-12-1-4218, NSF grant CMMI-1234585, and ONR grant N000141210719.

In this paper we consider the problem of selecting the optimal locations of a set of hubs $X = \{x_1, \ldots, x_k\}$ in a planar Euclidean region R where the "spokes" are continuously and uniformly distributed in the region; specifically, our optimization problem is given by

$$\underset{X}{\text{minimize}}\, \text{Fix}(|X|) + \phi\, \text{BBN}(X) + \psi\, \text{FW}(X, R) \tag{1}$$

where ϕ and ψ are given scalar parameters. Here the term $\text{Fix}(|X|) = \text{Fix}(k)$ represents the fixed costs and depends only on the number of elements of X, i.e. k (which is a decision variable), and not their geographic locations. The term $\phi\, \text{BBN}(X)$ represents the cost of the backbone network of the points X, which may be a Euclidean Steiner or minimum spanning tree (MST), a travelling salesman (TSP) tour, a star network (SN), a collection of capacitated vehicle routing (VRP) tours, a complete bipartite graph (CBG), or a complete graph (CG) on the points X. Finally, we define the *Fermat-Weber* cost function

$$\text{FW}(X, R) = \iint_R \min_i \{||x - x_i||\}\, dA\,, \tag{2}$$

where x is the variable of integration, the points x_i are the members of the hub set X, and dA denotes the area differential, to represent the local transportation costs incurred from providing service from the hubs X to the region R; the above quantity is simply proportional to the average distance between a point x uniformly sampled in R and its nearest hub point $x_i \in X$. This models the case where the "spokes" of the network are uniformly distributed in R and each spoke uses its nearest hub x_i by means of a direct trip. These three costs are illustrated in Figure 1, which shows the seven backbone network structures of interest and the Voronoi partition of the service region, which we include so as to suggest the local hub-to-spoke transportation costs.

The specific contributions of this paper are as follows: in our earlier manuscript [8], we have considered the special case of problem (1) where $\text{BBN}(\cdot) = \text{TSP}(\cdot)$ (and by extension, the cases where $\text{BBN}(\cdot) = \text{Steiner}(\cdot)$ and $\text{BBN}(\cdot) = \text{MST}(\cdot)$ as well). This paper extends that analysis to the other four cases $\text{BBN}(\cdot) \in \{\text{SN}(\cdot), \text{VRP}(\cdot), \text{CBG}(\cdot), \text{CG}(\cdot)\}$, deriving both the asymptotic behavior of the optimal solution in Part I and fast and simple approximation algorithms in Part II. Our approach here additionally allows us to quantify precisely what values of the input parameters affect the optimal cost and structure of the problem most significantly. In Section 5, we consider a further generalization of problem (1) in which the region R is serviced by a *multi-level* network in which network flows move through multiple levels of transshipment before reaching the service region. We derive asymptotic expressions that describe various properties of the optimal solution of such a multi-layer problem, such as the optimal number of points to place, their spatial distribution, and the optimal overall objective cost as a function of the region size and the relevant input parameters.

Related work

Our problem (1) can be seen as a particular instance of the *hub location problem* [6, 22, 36] in which we have a continuum of "spokes" in a planar region and we are permitted to choose a variety of backbone network topologies that connect our hubs. Another model closely related to (1) can be found in the seminal paper [25], which describes several discrete and continuous models and algorithms for simultaneous facility location and routing; further developments on discrete formulations of problems of this type have since emerged [1, 27, 28]. The recent paper [2] considers a discrete version of problem (1) where a Steiner tree of the facilities is used as a backbone network.

Our analysis here involves a planar version of an intrinsically discrete problem (in which we assume that demand is uniformly distributed in a region), and as such it falls in the company of such continuous approximation models as [6, 11, 13, 21, 24, 30, 42], the three-part series [31, 32, 33], and much of the material in the monograph [10]. The recent paper [5] considers a special case of (1), in which fixed costs are omitted and the backbone network cost function is a TSP tour of the points X, to estimate the "carbon penalty" of the emissions produced by a set of facilities (that is, the difference between the carbon cost to a firm and the true externality cost of the total emissions generated). The author shows that, using reasonable estimates of the input parameters, the realized penalty is negligible.

A relatively new branch in location theory deals with *location-routing* problems (LRP) that pay special attention to vehicle routing issues in facility placement [29]. Such problems are substantially more difficult than the canonical location models because, as the paper [4] observes,

> [T]he facility...must be "central" relative to the ensemble of the demand points, as ordered by the (yet unknown) tour through all of them. By contrast, in the classical problems the facility...must be located by considering distances to individual demand points, thus making the problem more tractable.

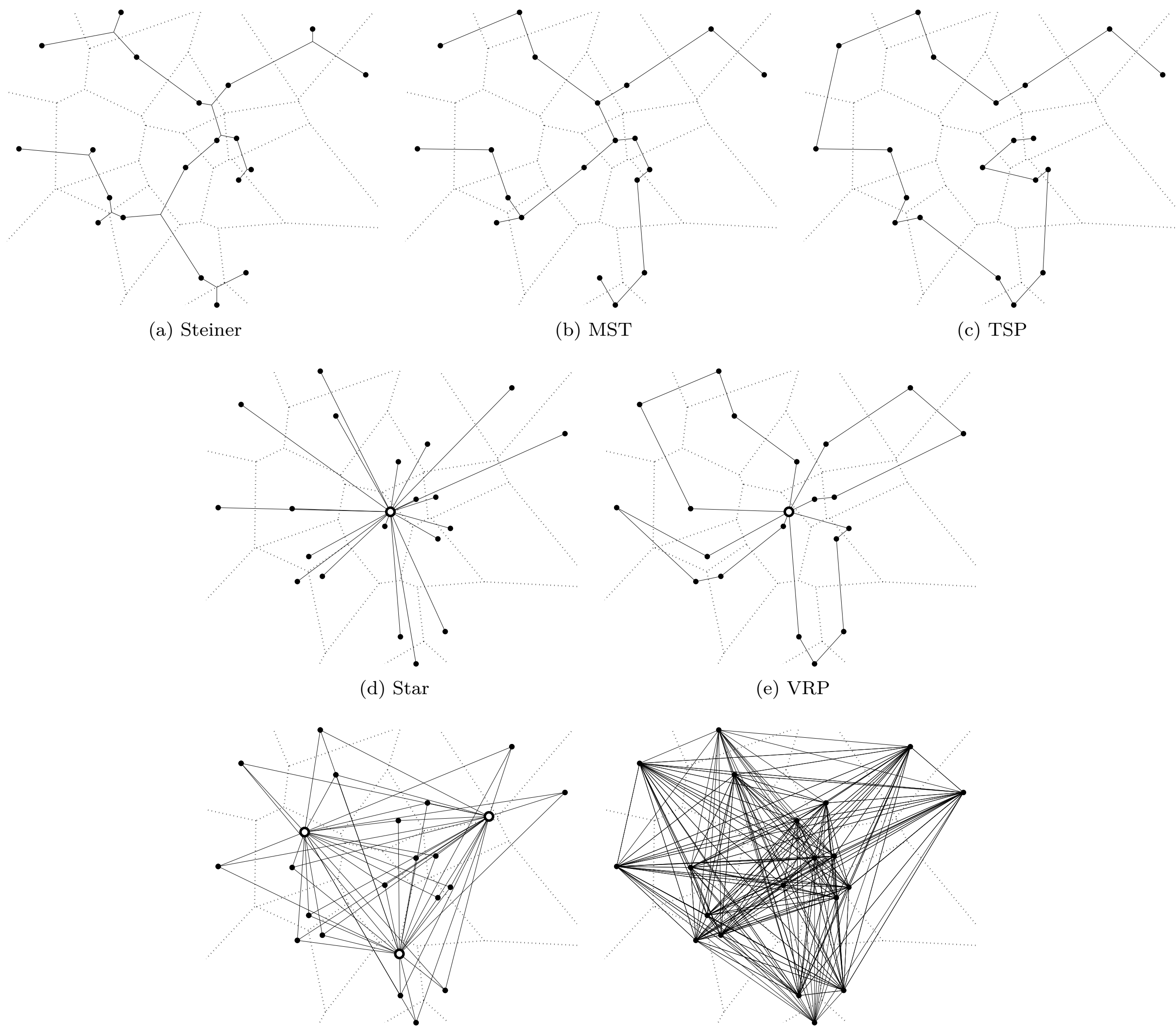

(a) Steiner (b) MST (c) TSP

(d) Star (e) VRP

(f) Complete bipartite graph (g) Complete graph

Figure 1: The seven backbone network structures considered in this paper for a fixed point set X, together with the induced Voronoi partition. Note that we have shown additional "root" or "depot" nodes in (1d)-(1f), as prescribed by their definitions.

One important distinction between the LRP and our problem (1) is that we think of the backbone network as connecting the *facilities* together, whereas the LRP considers networks that connect the *customers* together (i.e. vehicle tours that provide service to the customers).

Sections 2 and 4 of this paper concern the limiting behavior of the optimal solution to our problem (1) as the various input parameters of the objective function become large or small. As such, our analysis closely resembles other research on the asymptotic behavior of Euclidean optimization problems, such as the travelling salesman problem [3] and general *subadditive Euclidean functionals* [40, 44] as well as the k-*center* and k-*medians* problems [20, 49]. Although our analysis is deterministic (as opposed to the cited works which are probabilistic), the spirit of our contribution is most closely related to the aforementioned results.

Backbone network topologies

Before proceeding further, we find it useful to briefly give some context to the seven backbone network topologies that we study in this paper.

Steiner trees, MSTs, and TSPs The Steiner tree, minimum spanning tree, and travelling salesman tour are all *subadditive Euclidean functionals* [40, 44] whose lengths in a bounded region increase at a rate proportional to $\sqrt{k}$ in the worst case (here $k = |X|$ represents the number of hub points that we place). It is well-known [45] that the lengths of these configurations are always within a constant factor of each other; specifically, in Euclidean space, we have

$$\mathrm{Steiner}(X) \leq \mathrm{MST}(X) \leq \mathrm{TSP}(X) \leq 2\,\mathrm{Steiner}(X)\,.$$

In the context of hub location, backbone structures of this type are often called *corridor* or *fixed-route transportation networks* [19, 41, 46].

Star networks The discrete case of problem (1) with a star network $\mathrm{SN}(X)$ as a backbone structure is known as a "star-star" hub location problem [23] (because we have a star network that connects the hubs together as well as small-scale star networks that connect the hubs to spokes), which is commonly encountered in communication network design [37, 47] and satellite allocation [18]. Section 5.3.5 of the monograph [10] explains that such a network also occurs in air transportation of valuable goods because "the cost (and delay) of a stop is large compared with that of the moving portion of the trip." In the worst case, the length of the star network in a bounded region R increases at a rate proportional to k. In this paper, unless otherwise stated, we will assume that the root node of $\mathrm{SN}(X)$ is the geometric median of X, which we write as $\bar{x}$ (this allows us to treat the points of X homogeneously, i.e. to not identify a distinct "root node" and treat it separately from the others).

VRP tours A *VRP tour* of the points X is a generalization of the TSP tour in which vehicles depart from a central depot and visit the points X. The vehicle, however, is now *capacitated*: it can only visit a given number of stops κ before it is required to return to the depot. We therefore see that the TSP tour and the star network are special cases of the VRP tour in which $\kappa = \infty$ and $\kappa = 1$ respectively. Such a distribution model is canonical in a wide variety of contexts for modelling "one-to-many" relationships; see for example Chapter 4 of [10].

Complete bipartite graphs The *complete bipartite graph* is a "many-to-many" backbone structure that arises when our facilities X are interconnected with a second set of facilities Y. This might arise in a supply chain in which each facility $y_j \in Y$ produces a specific component that is used to construct a product at each facility x_i. Since components from *each* facility y_j are needed to construct the product, we must therefore connect each facility $y_j \in Y$ to each facility $x_i \in X$. Distribution networks of this type are sometimes referred to as *point-to-point* networks [41]. In the worst case, the length of a complete bipartite graph in a bounded region R increases at a rate proportional to $k_1 k_2$, where $k_1 = |X|$ and $k_2 = |Y|$.

Complete graphs The *complete graph* $\mathrm{CG}(X)$ is the most frequently used backbone structure in hub location problems [7] and is commonly encountered in airline network design [22], freight delivery [35], and urban transportation [34]. In the worst case, the length of the complete graph in a bounded region R increases at a rate proportional to k^2.

Notational conventions

In this paper we adopt the following notational conventions: we use $|X|$ to denote the cardinality of a set X, we let $\lfloor t \rfloor$, $\lceil t \rceil$, and $\lfloor t \rceil$ denote the floor, ceiling, and rounding functions of a real number t, we let $\mathrm{diam}(R) = \max_{x,y\in R} \|x - y\|$ denote the *diameter* of a region R, we let $N_\epsilon(x)$ denote an ϵ-neighborhood of a point x (or a set of points X), and we let $\mathrm{AR}(R)$ denote the *aspect ratio* of a rectangle R, i.e. the ratio of the longer side to the shorter side. When Q is a (possibly infinite) set of points, we define the distance function

$$d(x, Q) = \min_{q\in Q} ||x - q|| \,.$$

As mentioned in the previous section, we use $\bar{x}$ to denote the geometric median of the point set X, which we assume to be the root node of any star network $\mathrm{SN}(X)$ or VRP tour $\mathrm{VRP}(X)$ that we come across unless otherwise stated. We use the letter c as a generic constant that may change from one expression to the next; constants with numerical subscripts (such as α_1 in the next section) are those with a more permanent existence.

We previously defined the Fermat-Weber function $\mathrm{FW}(X, R)$ in (2), which models the cost of serving region R with the facilities X via direct trips. We will also define a function $\mathrm{FW}(R)$, which does not depend on any point set, as

$$\mathrm{FW}(R) = \min_{x_0\in R} \iint_R \|x - x_0\| \, dA \,,$$

so that x_0 ends up being the geometric median of the region R. We will commit a minor abuse of notation by using the terms $\mathrm{BBN}(\cdot)$, $\mathrm{Steiner}(\cdot)$, $\mathrm{MST}(\cdot)$, $\mathrm{TSP}(\cdot)$, $\mathrm{SN}(\cdot)$, $\mathrm{VRP}(\cdot)$, $\mathrm{CBG}(\cdot)$, and $\mathrm{CG}(\cdot)$ to refer both to the various backbone networks and to their lengths. Note that, in the above integral, we have used x as a variable of integration and dA to denote the area differential; we will maintain this convention throughout.

Finally, we shall make use of four common conventions in asymptotic analysis:

- We say that $f(x) \in \Omega(g(x))$ if there exists a positive constant c and a value x_0 such that $f(x) \geq c \cdot g(x)$ for all $x \geq x_0$,
- We say that $f(x) \in \mathcal{O}(g(x))$ if there exists a positive constant c and a value x_0 such that $f(x) \leq c \cdot g(x)$ for all $x \geq x_0$,
- We say that $f(x) \sim g(x)$ if $\lim_{x\to\infty} f(x)/g(x) = 1$, and
- We say that $f(x) \propto g(x)$ if there exist positive constants c_1 and c_2 and a value x_0 such that $c_1 g(x) \leq f(x) \leq c_2 g(x)$ for all $x \geq x_0$.

Part I
Asymptotic analysis

2 Special cases of (1)

In this section, we will examine the optimal solutions to certain special cases of problem (1). Before doing anything else, we find it useful to state a classical result of continuous location theory proven in [16], as well as an immediate corollary thereof:

Theorem 1. *If R is a bounded region in the plane with area (i.e. Lebesgue measure) A, then*

$$\inf_{X:|X|=k} \mathrm{FW}(X, R) \sim \frac{\alpha_1 A^{3/2}}{\sqrt{k}}$$

as $k \to \infty$, where $X = \{x_1, \ldots, x_k\}$ denotes a finite subset of $\mathbb{R}^2$ and α_1 is the Fermat-Weber value of a regular hexagon with unit area:

$$\alpha_1 = \mathrm{FW}\,(\mathrm{Hexagon}) = \frac{3^{3/4}\,(4 + 3\log 3)\,\sqrt{6}}{108} \approx 0.37721\,.$$

Theorem 1 says that, for sufficiently large point sets X, the optimal configuration that minimizes $\mathrm{FW}(X, R)$ is always a regular hexagonal lattice, i.e. the "honeycomb heuristic" [13, 20, 39], which is shown in Figure 3a. The paper [16] actually generalizes Theorem 1 to a more versatile setting in which, rather than minimizing the quantity

$$\mathrm{FW}(X, R) = \iint_R \min_i \{||x - x_i||\}\, dA\,,$$

we are interested in minimizing quantities of the more general form

$$\mathrm{FW}_f(X, R) := \iint_R \min_i \{f(||x - x_i||)\}\, dA\,,$$

where $f(\cdot) : [0, \infty) \to [0, \infty)$ is a monotonically increasing function:

Theorem 2. *If R is a bounded region in the plane with area (i.e. Lebesgue measure) A, and $f(\cdot) : [0, \infty) \to [0, \infty)$ is a monotonically increasing function, then*

$$\inf_{X : |X| = k} \mathrm{FW}_f(X, R) \sim k \cdot \mathrm{FW}_f(\mathrm{Hex}(A/k))$$

as $k \to \infty$, where $X = \{x_1, \ldots, x_k\}$ denotes a finite subset of $\mathbb{R}^2$, $\mathrm{Hex}(A/k)$ denotes a regular hexagon of area A/k, and

$$\mathrm{FW}_f(\mathrm{Hex}(A/k)) := \iint_{\mathrm{Hex}(A/k)} f(\|x - x_0\|)\, dA$$

where x_0 is the centroid of the hexagon in question.

Simply put, Theorem 2 says that the honeycomb heuristic is an asymptotically optimal configuration whenever our objective is to minimize any monotonically increasing *function* of the distances from the landmark points x_i to the region R. This will be useful to us in Section 5 when we analyze hub-and-spoke networks with multiple levels.

2.1 The case $\phi = 0$: the honeycomb heuristic

Before studying our problem (1) for various forms of $\mathrm{BBN}(\cdot)$, we remark that it is obvious that the solution to (1) when backbone network costs are ignored, i.e.

$$\underset{X}{\text{minimize}}\ \mathrm{Fix}(|X|) + \psi\, \mathrm{FW}(X, R)\,, \tag{3}$$

is the honeycomb heuristic. In particular, provided the optimal number of points X to place is sufficiently large (which would happen as $\psi \to \infty$), we can apply Theorem 1 to obtain a nearly optimal solution by minimizing the expression

$$\mathrm{Fix}(k) + \frac{\psi \alpha_1}{\sqrt{k}} \tag{4}$$

over k.

2.2 The case $\mathrm{Fix}(\cdot) = 0$ and $\mathrm{BBN}(\cdot) \in \{\mathrm{Steiner}(\cdot), \mathrm{MST}(\cdot), \mathrm{TSP}(\cdot)\}$: the Archimedes heuristic

If $\mathrm{Fix}(k) = 0$ for all k, then we do not incur any penalty for placing hubs in the region if they do not lengthen the backbone network. Thus, when $\mathrm{BBN}(\cdot) \in \{\mathrm{Steiner}(\cdot), \mathrm{MST}(\cdot), \mathrm{TSP}(\cdot)\}$, our optimal configuration will be to place infinitely many hubs along the backbone network (see Figure 2), although we have not yet discussed what the shape of the backbone network should be. We can derive the optimal shape by proving the following lemma:

Lemma 3. *Suppose that T is a tree in a region R such that* $\mathrm{length}(T) = \ell$ *and* $\mathrm{Area}(R) = A$. *Then* $\mathrm{FW}\,(T, R) \geq \frac{2A^2}{8\ell + 3\sqrt{\pi A}}$.

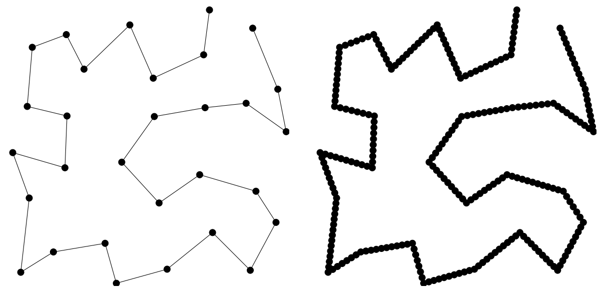

(a) (b)

Figure 2: If $\mathrm{Fix}(k) = 0$ for all k, then the absence of fixed costs for hubs implies that configuration (2a) is strictly worse than (2b); that is, we should place infinitely many hubs along the backbone network to maximize network utilization.

Proof. See Section A of the Online Supplement. For ease of intuition, we can show that $\mathrm{FW}(T, R) \in \Omega(1/\ell)$ if $A = 1$: we observe that the area of a neighborhood $N_\epsilon(T)$ of T with radius $\epsilon = {}^{1}\!/\!{}_{4\ell}$ is approximately $1/2$, and therefore there exists an area of approximately $1/2$ lying outside that neighborhood, i.e. $\mathrm{Area}(R \setminus N_\epsilon(T)) \approx 1/2$. Every point lying outside this neighborhood is at a distance of at least ${}^{1}\!/\!{}_{4\ell}$ away from T and therefore the Fermat-Weber value $\mathrm{FW}(T, R)$ is approximately bounded below by $(1/2)({}^{1}\!/\!{}_{4\ell}) = {}^{1}\!/\!{}_{8\ell}$. □

The optimal solution to problem (1) is then described by the following:

Theorem 4. *As $\phi/\psi \to 0$, the optimal solution X^* to the problem*

$$\underset{X}{\text{minimize}}\, \phi\, \mathrm{BBN}(X) + \psi\, \mathrm{FW}(X, R)$$

with $\mathrm{BBN}(\cdot) \in \{\mathrm{Steiner}(\cdot), \mathrm{MST}(\cdot), \mathrm{TSP}(\cdot)\}$ *satisfies*

$$\phi\, \mathrm{BBN}(X^*) + \psi\, \mathrm{FW}(X^*, R) \sim A\sqrt{\phi\psi}$$

where $A = \mathrm{Area}(R)$*. Moreover, an optimal solution X^* is the* Archimedean spiral *configuration, as shown in Figure 3b.*

Proof. Using Lemma 3, we can determine a lower bound for the problem

$$\underset{X}{\text{minimize}}\, \phi\, \mathrm{BBN}(X) + \psi\, \mathrm{FW}(X, R) \tag{5}$$

via

$$\min_{\ell}\, \phi\ell + \psi \frac{2A^2}{8\ell + 3\sqrt{\pi A}}$$

which is minimized at $\ell^* = \max\{{}^{A}\!/\!{}_{2}\sqrt{\psi/\phi} - {}^{3}\!/\!{}_{8}\sqrt{\pi A}, 0\}$. Since we are performing an asymptotic analysis as $\phi/\psi \to 0$, we are free to assume that $\ell^* = {}^{A}\!/\!{}_{2}\sqrt{\psi/\phi} - {}^{3}\!/\!{}_{8}\sqrt{\pi A}$, at which point the objective function evaluates to

$$\phi\ell^* + \psi \frac{2A^2}{8\ell^* + 3\sqrt{\pi A}} = A\sqrt{\phi\psi} - \frac{3\sqrt{\pi A}}{8}\phi \sim A\sqrt{\phi\psi} \text{ as } \phi/\psi \to 0\,.$$

We conclude by observing that if we configure an infinite number of hubs X on an Archimedean spiral of the form $r = a\theta$ in polar coordinates, where $a = \sqrt{\phi/\psi}/\pi$, then for a sufficiently small ratio ϕ/ψ we have $\phi\, \mathrm{BBN}(X) + \psi\, \mathrm{FW}(X, R) \sim A\sqrt{\phi\psi}$, thus proving that the Archimedes heuristic is an optimal configuration for minimizing (5) when we use a Steiner tree, MST, or TSP tour of X as a backbone network.

□

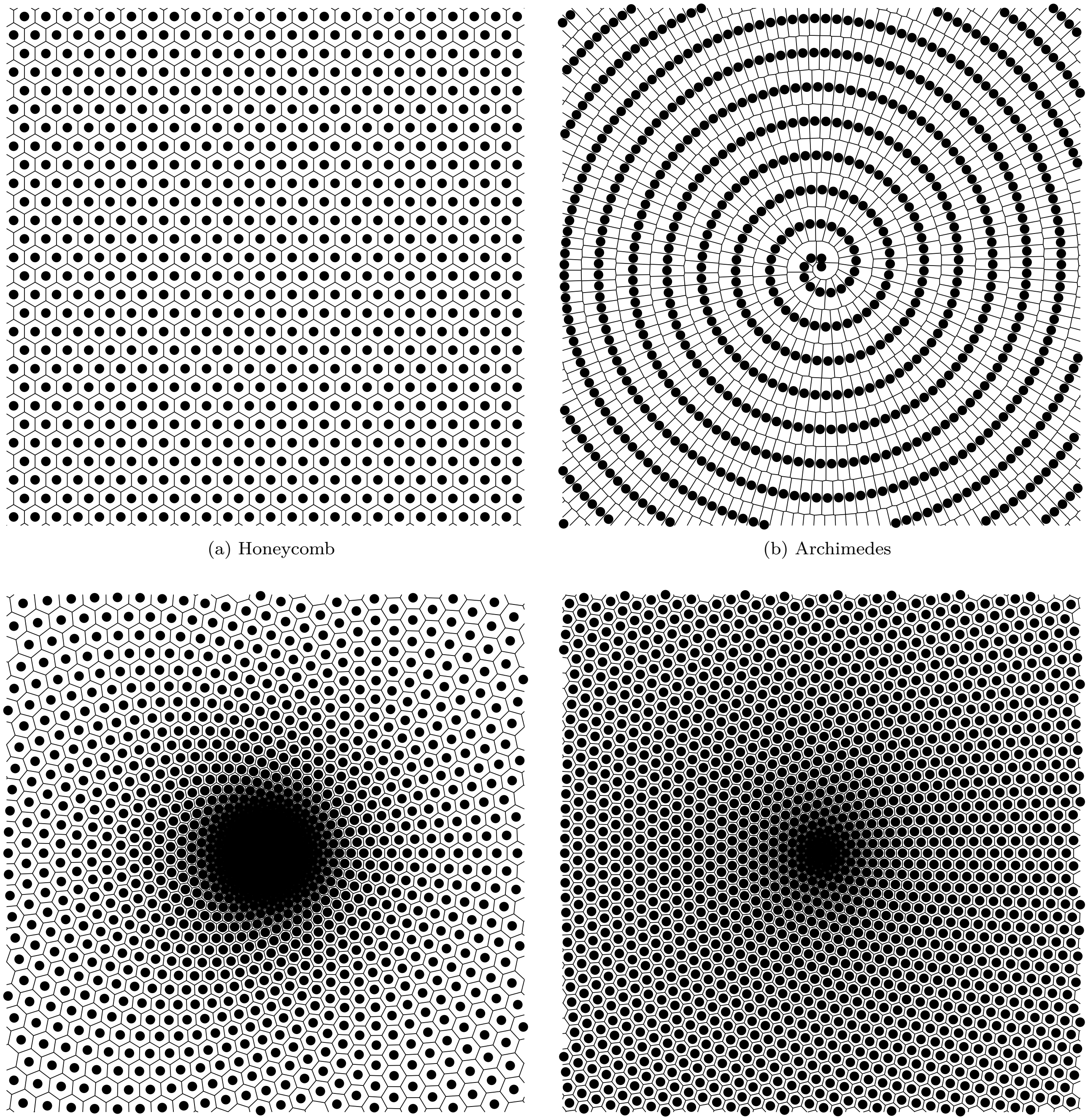

(a) Honeycomb

(b) Archimedes

(c) "Contracted honeycomb"

(d) "Less contracted honeycomb"

Figure 3: Optimal configurations for four of the special instances of (1) described throughout Section 2 and their Voronoi diagrams.

2.3 The case $\mathrm{Fix}(\cdot) = 0$ and $\mathrm{BBN}(\cdot) = \mathrm{SN}(\cdot)$: the "contracted honeycomb"

We next consider the case where (1) takes the form

$$\underset{X}{\text{minimize}}\,\phi\,\mathrm{SN}(X) + \psi\,\mathrm{FW}(X,R)\,. \tag{6}$$

It is clear that, as $\phi/\psi \to \infty$, the optimal solution to (6) involves placing fewer and fewer facilities throughout the region because the backbone network costs dominate the local transportation costs. We therefore consider instead the case where $\phi/\psi \to 0$, whose optimal solution is characterized by the following theorem:

Theorem 5. *As $\phi/\psi \to 0$, the optimal solution X^* to problem* (6) satisfies

$$\phi\,\mathrm{SN}(X^*) + \psi\,\mathrm{FW}(X^*,R) \sim cA^{7/6}\phi^{1/3}\psi^{2/3}\,,$$

where $A = \mathrm{Area}(R)$ and c is a constant that depends only on the shape of the region R. Moreover, the optimal solution X^* is a "contracted honeycomb" configuration that follows the distribution $f(x) = c^{'}\|x\|^{-2/3}$ on R for a suitable constant $c^{'}$, as shown in Figure 3c.

Proof sketch. Suppose without loss of generality that the center of the star network $\bar{x} \in R$ is the origin, and that we divide R into N cells $\square_i$ of size $\epsilon = A/N$. Let $d_i = \min_{x\in\square_i}\|x\|$ and let the variable $k_i = |X \cap \square_i|$ denote the number of points in $\square_i$ (so that $k = \sum_{i=1}^N k_i$). Consider a particular cell $\square_i$: as $\phi/\psi \to 0$, it must be true that the optimal number of points k_i^* in $\square_i$ increases. Thus, for sufficiently large k_i, Theorem 1 says that

$$\min_{X_i:|X_i|=k_i} \mathrm{FW}(X_i,\square_i) \sim \frac{\alpha_1\epsilon^{3/2}}{\sqrt{k_i}}\,.$$

We therefore find that, as $\phi/\psi \to 0$, a lower bound of (6) is given by solving

$$\underset{(k_1,\dots,k_N)}{\text{minimize}}\,\underbrace{\phi\sum_{i=1}^N d_ik_i}_{\le \mathrm{SN}(X)} + \underbrace{\psi\,\alpha_1\epsilon^{3/2}\sum_{i=1}^N\frac{1}{\sqrt{k_i}}}_{\le \mathrm{FW}(X,R)}\,.$$

The above problem is convex in $(k_1,\dots,k_N)$. Setting first derivatives to zero, we find that for each i we must have

$$\phi d_i = \frac{1}{2}\cdot\frac{\psi\alpha_1\epsilon^{3/2}}{k_i^{3/2}}\,.$$

Introducing a variable $f_i := {}^{k_i}/_{\epsilon k}$, the above can equivalently be written as

$$f_i = (\alpha_1/2)^{2/3}\cdot\frac{(\psi/\phi)^{2/3}}{d_i^{2/3}k}$$

which is simply a finite discretization of the expression

$$f(x) = (\alpha_1/2)^{2/3}\cdot\frac{(\psi/\phi)^{2/3}}{\|x\|^{2/3}k}$$

where $f(x)$ describes the "density" of the points X. Introducing $c^{'} = (\alpha_1/2)^{2/3}(\psi/\phi)^{2/3}/k$, the above can equivalently be written as

$$f(x) = c^{'}\|x\|^{-2/3}\,.$$

This tells us that as k becomes large, the optimal X that minimizes (6) is a "contracted honeycomb" configuration: we define $c^{'} = \left(\iint_R \|x\|^{-2/3}\,dA\right)^{-1}$ and then place a total of $k = (\alpha_1/2)^{2/3}(\psi/\phi)^{2/3}/c^{'}$ points in R in a honeycomb configuration that follows the distribution $f(x) = c^{'}\|x\|^{-2/3}$ on R. Note that the optimal number of points k is proportional to $(\psi/\phi)^{2/3}$, the backbone network cost is

$$\phi \sum_{i=1}^{N} d_i k_i \sim \left(\frac{\alpha_1}{2}\right)^{2/3} \left(\iint_R \|x\|^{1/3}\, dA\right) \phi^{1/3}\psi^{2/3}\,, \tag{7}$$

and the coverage cost is

$$\psi\alpha_1\epsilon^{3/2}\sum_{i=1}^{N}\frac{1}{\sqrt{k_i}} \sim \left(2^{1/3}\alpha_1^{2/3}\right)\left(\iint_R \|x\|^{1/3}\, dA\right)\phi^{1/3}\psi^{2/3}\,.$$

If we assume that the shape of R is fixed, we see that $\iint_R \|x\|^{1/3}\, dA \propto A^{7/6}$, so that the optimal objective function value is proportional to $A^{7/6}\phi^{1/3}\psi^{2/3}$. This completes the proof. $\square$

Remark 6. It is worth noting that as $\phi/\psi \to 0$, the optimal number of points k varies but the overall spatial distribution $f(x) = c^{'}\|x\|^{-2/3}$ does not. Practically speaking, this a useful property of the star network because, if ϕ decreases (or conversely if ψ increases), we can improve our objective value by simply placing additional points distributed according to $f(x)$, rather than having to start from scratch. The same cannot be said of the optimal solution when the backbone network is a Steiner tree, MST, or TSP – i.e. the Archimedes heuristic – which becomes more tightly "coiled" as $\phi/\psi \to 0$.

2.4 The case $\mathrm{Fix}(\cdot) = 0$ and $\mathrm{BBN}(\cdot) = \mathrm{VRP}(\cdot)$

A *VRP tour* of the points X is a generalization of the TSP tour in which vehicles depart from a central depot $\bar{x}$ (which we will again assume to be the origin) and visit the points X. The vehicle, however, is now *capacitated*: it can only visit a given number of stops κ before it is required to return to the depot. We therefore see that the TSP tour and the star network are special cases of the VRP tour in which $\kappa = \infty$ and $\kappa = 1$ respectively. We will consider here the case where (1) takes the form

$$\underset{X}{\text{minimize}}\, \phi\, \mathrm{VRP}(X) + \psi\, \mathrm{FW}(X, R)\,. \tag{8}$$

The paper [17] proves that, for any point set X, we have

$$\max\left\{\mathrm{TSP}(X), \frac{2}{\kappa}\,\mathrm{SN}(X)\right\} \le \mathrm{VRP}(X) \le 2\left\lceil\frac{|X|}{\kappa}\right\rceil \cdot \frac{\mathrm{SN}(X)}{|X|} + (1 - 1/\kappa)\,\mathrm{TSP}(X)\,. \tag{9}$$

We will disregard the upper bounds of $\mathrm{VRP}(X)$ for now. The fact that $\mathrm{VRP}(X) \ge \mathrm{TSP}(X)$ allows us to immediately conclude (owing to the result of Section 2.2) that a valid asymptotic lower bound of (8) as $\phi/\psi \to 0$ is $A\sqrt{\phi\psi}$. Similarly, the fact that $\mathrm{VRP}(X) \ge {}^2/_\kappa\, \mathrm{SN}(X)$ allows us to conclude (owing to the result of Section 2.3) that another valid asymptotic lower bound of (8) is

$$\underbrace{\left(2^{2/3} + 2^{-1/3}\right)\alpha_1\left(\iint_R \|x\|^{1/3}\, dA\right)}_{=:cA^{7/6}}\left(\frac{\phi}{\kappa}\right)^{1/3}\psi^{2/3}\,.$$

Some simple algebra shows that the two lower bounds are equal when $\kappa = c^3\sqrt{A\psi/\phi}$. Moreover, as κ becomes small relative to $c^3\sqrt{A\psi/\phi}$, we find that $\mathrm{VRP}(X) \sim {}^2/_\kappa\, \mathrm{SN}(X)$, and as κ becomes large relative to $c^3\sqrt{A\psi/\phi}$, we find that $\mathrm{VRP}(X) \sim \mathrm{TSP}(X)$ (this follows from the analysis in [17]). Thus, when $\kappa \ll c^3\sqrt{A\psi/\phi}$, we find that a "contracted honeycomb" configuration becomes optimal (i.e. treating our problem as that of Section 2.3, making the substitution $\phi \mapsto {}^2/_\kappa \cdot \phi$), and when $\kappa \gg c^3\sqrt{A\psi/\phi}$, the Archimedes heuristic becomes optimal (with the same coefficients ϕ and ψ).

2.5 The case $\mathrm{Fix}(\cdot) = 0$ and $\mathrm{BBN}(\cdot) = \mathrm{CBG}(\cdot)$

When the backbone network is a complete bipartite graph, we have an additional set of hub nodes Y and our problem takes the form

$$\underset{X}{\text{minimize}}\, \phi\, \mathrm{CBG}(X, Y) + \psi\, \mathrm{FW}(X, R) \tag{10}$$

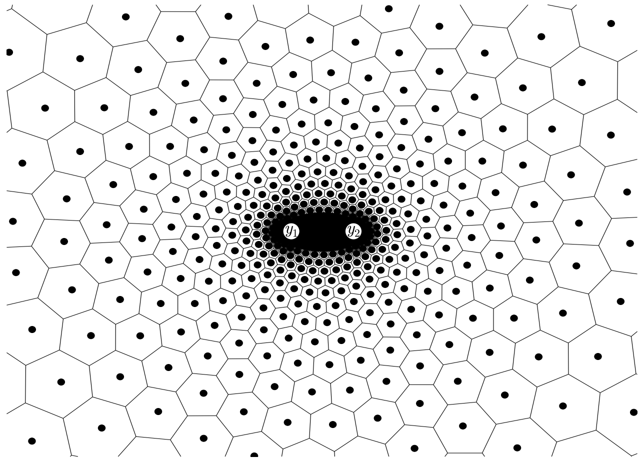

Figure 4: A contracted honeycomb configuration derived for a complete bipartite graph with $|Y| = 2$.

where we define

$$\mathrm{CBG}(X, Y) = \sum_{i=1}^{|X|} \sum_{j=1}^{|Y|} \|x_i - y_j\| .$$

Note that in (10) we are only treating X as an optimization variable and assuming that Y is exogenous. This is because, if Y were an optimization variable as well, the optimal solution to (10) would be to set $Y = \emptyset$, thus incurring no backbone network costs whatsoever. When Y is given and fixed, we simply have a generalization of problem (6) in which we define

$$c^{'} = \left[\iint_R \left(\sum_{j=1}^{|Y|} \|x - y_j\| \right)^{-2/3} dA \right]^{-1}$$

and then place a total of $k = (\alpha_1/2)^{2/3}(\psi/\phi)^{2/3}/c^{'}$ points in R in a honeycomb configuration that follows the distribution

$$f(x) = c^{'} \left(\sum_{j=1}^{|Y|} \|x - y_j\| \right)^{-2/3}$$

on R. The optimal objective function value is again proportional to $A^{7/6}\phi^{1/3}\psi^{2/3}$. Figure 4 shows a picture of this configuration for the case where $|Y| = 2$.

2.6 The case $\mathrm{Fix}(\cdot) = 0$ and $\mathrm{BBN}(\cdot) = \mathrm{CG}(\cdot)$: the "less contracted honeycomb"

When (1) takes the form

$$\underset{X}{\text{minimize}}\, \phi\, \mathrm{CG}(X) + \psi\, \mathrm{FW}(X, R)\,, \tag{11}$$

it is difficult to determine a closed-form solution for the optimal configuration of the facilities X as in the previous examples, although it is straightforward to find a solution whose objective value is guaranteed to fall within roughly 15% of the optimum. It is clear that, as $\phi/\psi \to \infty$, the optimal solution to (11) involves placing fewer and fewer facilities in the region because the backbone network costs dominate the local transportation costs. We therefore again consider instead the case where $\phi/\psi \to 0$, whose optimal solution is characterized by the following:

Theorem 7. *As $\phi/\psi \to 0$, the optimal solution X^* to problem (11) satisfies*

$$\phi\, \mathrm{CG}(X^*) + \psi\, \mathrm{FW}(X^*, R) \propto A^{13/10}\phi^{1/5}\psi^{4/5}$$

where $A = \text{Area}(R)$. Moreover, an approximately optimal solution X^{**} is a "less contracted honeycomb" configuration that follows the distribution $f(x) = c^{'}(\|x\| + c^{''})^{-2/3}$ on R for suitable constants $c^{'}$ and $c^{''}$, as shown in Figure 3d; such a configuration is guaranteed to have an objective value that falls within $2^{1/5} - 1 \approx 15\%$ of the optimum.

Proof sketch. Let $\bar{x}$ denote the geometric median of X. By definition, we have

$$\sum_{j=1}^{k} \|\bar{x} - x_j\| \leq \sum_{j=1}^{k} \|x - x_j\| \quad \forall x \in R$$

and so in particular, for any point $x_i \in X$, we have $\sum_{j=1}^{k} \|\bar{x} - x_j\| \leq \sum_{j=1}^{k} \|x_i - x_j\|$. It follows that

$$\text{CG}(X) = \frac{1}{2} \sum_{i=1}^{k} \sum_{j=1}^{k} \|x_i - x_j\| \geq \frac{1}{2} \sum_{i=1}^{k} \sum_{j=1}^{k} \|\bar{x} - x_j\| = \frac{k}{2} \sum_{j=1}^{k} \|\bar{x} - x_j\| = \frac{k}{2} \text{SN}(X)\,.$$

However, by the triangle inequality, it also holds that

$$\text{CG}(X) \leq \frac{1}{2} \sum_{i=1}^{k} \sum_{j=1}^{k} \|x_i - \bar{x}\| + \|\bar{x} - x_j\| = k\,\text{SN}(X)$$

so that ${}^{k}\!/_{2} \cdot \text{SN}(X) \leq \text{CG}(X) \leq k \cdot \text{SN}(X)$. Thus, we can find an upper bound to problem (11) by solving

$$\underset{X}{\text{minimize}}\, \phi k\, \text{SN}(X) + \psi\, \text{FW}(X, R) \tag{12}$$

where $k = |X|$ is also a variable as before. Treating this problem in precisely the same manner as Section 2.3, and assuming that $\bar{x}$ is the origin, we find that the optimal "density" $f(\cdot)$ of the points that minimizes (12) must satisfy

$$\phi k^{5/2} \left(\|x\| + \iint_R \|x\| f(x)\, dA \right) = \frac{1}{2} \cdot \frac{\psi \alpha_1}{f(x)^{3/2}}$$

i.e.

$$f(x) = k^{-5/3} (\alpha_1/2)^{2/3} \, (\psi/\phi)^{2/3} \left(\|x\| + \iint_R \|x\| f(x)\, dA \right)^{-2/3}.$$

Finally, introducing c such that $k = \frac{\psi^{2/5}}{c^{3/5} \phi^{2/5}}$, we can write

$$\begin{aligned} f(x) &= \underbrace{c(\alpha_1/2)^{2/3}}_{c'} \left(\|x\| + \underbrace{\iint_R \|x\| f(x)\, dA}_{c''} \right)^{-2/3} \\ &= c^{'} \left(\|x\| + c^{''} \right)^{-2/3} \end{aligned} \tag{13}$$

so that we merely need to find constants $c^{'}$ and $c^{''}$ such that

$$\iint_R c^{'} \left(\|x\| + c^{''} \right)^{-2/3} dA = 1 \tag{14}$$

$$\iint_R c^{'} \left(\|x\| + c^{''} \right)^{-2/3} \|x\|\, dA = c^{''}\,. \tag{15}$$

We thus find that the approximately optimal solution to (11) is to distribute a total of $k = \frac{\psi^{2/5}}{c^{3/5} \phi^{2/5}}$ hub points in a honeycomb lattice that follows the distribution $f(x) = c^{'}(\|x\| + c^{''})^{-2/3}$ for appropriate constants c, $c^{'}$ and $c^{''}$. This

Objective function	Optimal configuration	Optimal objective value
$\mathrm{Fix}(\lvert X\rvert) + \psi\,\mathrm{FW}(X,R)$	Honeycomb	Depends on $\mathrm{Fix}(\cdot)$
$\phi\,\mathrm{Steiner}(X) + \psi\,\mathrm{FW}(X,R)$	Archimedes	$\propto A\sqrt{\phi\psi}$
$\phi\,\mathrm{MST}(X) + \psi\,\mathrm{FW}(X,R)$	Archimedes	$\propto A\sqrt{\phi\psi}$
$\phi\,\mathrm{TSP}(X) + \psi\,\mathrm{FW}(X,R)$	Archimedes	$\propto A\sqrt{\phi\psi}$
$\phi\,\mathrm{SN}(X) + \psi\,\mathrm{FW}(X,R)$	Contracted honeycomb	$\propto A^{7/6}\phi^{1/3}\psi^{2/3}$
$\phi\,\mathrm{VRP}(X) + \psi\,\mathrm{FW}(X,R)$	$\kappa \ll c^3\sqrt{A\psi/\phi}$: Contracted honeycomb $\kappa \gg c^3\sqrt{A\psi/\phi}$: Archimedes	$\propto A^{7/6}\phi^{1/3}\psi^{2/3}/\kappa^{1/3}$ $\propto A\sqrt{\phi\psi}$
$\phi\,\mathrm{CBG}(X) + \psi\,\mathrm{FW}(X,R)$	Contracted honeycomb	$\propto A^{7/6}\phi^{1/3}\psi^{2/3}$
$\phi\,\mathrm{CG}(X) + \psi\,\mathrm{FW}(X,R)$	Less contracted honeycomb	$\propto A^{13/10}\phi^{1/5}\psi^{4/5}$

Table 1: Summary of the major results from Section 2. In the row corresponding to the case where $\mathrm{BBN}(\cdot) = \mathrm{VRP}(\cdot)$, the value κ is the vehicle capacity and the value c is a quantity derived from the shape of the service region R (see Section 2.4).

configuration is shown in Figure 3d. Note that the optimal number of points k is proportional to $(\psi/\phi)^{2/5}$, the backbone network cost approaches

$$\phi k \sum_{i=1}^{N} d_i k_i \sim \left[\frac{1}{c^{6/5}} \cdot \iint_R c^{'}(\|x\| + c^{''})^{-2/3}\|x\|\,dA\right] \phi^{1/5}\psi^{4/5} \text{ as } \phi/\psi \to 0\,, \tag{16}$$

and the coverage cost approaches

$$\psi\alpha_1\epsilon^{3/2}\sum_{i=1}^{N}\frac{1}{\sqrt{k_i}} \sim \left[\frac{2}{c^{6/5}} \cdot \iint_R c^{'}\left(\|x\| + c^{''}\right)^{1/3} dA\right] \phi^{1/5}\psi^{4/5} \text{ as } \phi/\psi \to 0\,.$$

If we assume that the shape of R is fixed, we see that the optimal objective function value is proportional to $A^{13/10}\phi^{1/5}\psi^{4/5}$. Note that a lower bound of our problem is obtained by solving

$$\underset{X}{\mathrm{minimize}}\,\phi\left(\frac{k}{2}\right)\mathrm{SN}(X) + \psi\,\mathrm{FW}(X,R)$$

which has an objective function value within a factor of $2^{1/5} \approx 1.15$ of the upper bound that we just computed. $\square$

Remark 8. Similarly to Remark 6, it is worth noting that as $\phi/\psi \to 0$, the near-optimal number of points k varies but the overall spatial distribution $f(x) = c^{'}(\|x\| + c^{''})^{-2/3}$ does not.

2.7 Summary table

We summarize the major results of this section in Table 1.

3 A practical example

Before extending the results of Section 2, we find it helpful to first give a practical example using parameter estimates taken from the existing literature. Suppose that we are to provide service to a circular geographic region of 100 square miles containing 150 customers that are uniformly distributed throughout. Our goal is to transport goods from a supply depot that is initially located in the center of the region to a set of transshipment nodes (whose locations we will determine) along to our customers. We are to accomplish this using a combination of large, high-efficiency electric trucks to transport goods from the depot to the transshipment nodes, together with smaller gasoline-powered vans for transportation to the customers. We can calculate the cost per mile for transportation along the backbone network for the Smith Newton all-electric truck using the estimates in Tables 1 and 4 of [12], which gives

$$\frac{80 \text{ kW h}}{100 \text{ miles}} \cdot \frac{\$0.1106}{\text{kW h}} = \frac{\$0.0885}{\text{mile}} =: \phi' \,.$$

The cost per mile for an all-purpose van such as the Suzuki APV can similarly be estimated via

$$\frac{1 \text{ gallon}}{25 \text{ miles}} \cdot \frac{\$3.603}{1 \text{ gallon}} = \frac{\$0.1441}{\text{mile}} =: \psi' \,.$$

Our reason for using the notation "ϕ'" and "ψ'" will be clear shortly. We will assume that the large electric trucks deliver goods from the central depot to the transshipment nodes by way of direct trips and that the small vans also deliver goods from the transshipment nodes to the customers by way of direct trips (see Section 5.3.5 of [10] for an explanation of the circumstances that result in such a scenario). Thus, if X denotes the set of transshipment nodes, we find that the cost of the backbone network is $2\phi' \,\mathrm{SN}(X) =: \phi \,\mathrm{SN}(X)$, where the multiplier "2" is used because we are making round trips to and from the transshipment nodes. Since the small vans are also providing service via direct trips, and since there are 150 customers distributed in 100 square miles, we see that the total workload of the small vans is

$$2\psi' \frac{150}{100} \,\mathrm{FW}(X, R) =: \psi \,\mathrm{FW}(X, R) \,.$$

Our problem is then given by

$$\underset{X}{\text{minimize}} \, \phi \,\mathrm{SN}(X) + \psi \,\mathrm{FW}(X, C)$$

with $\phi = 0.1770$ and $\psi = 0.4324$. The solution is to define $c' = \left(\iint_R \|x\|^{-2/3} \, dA\right)^{-1}$ and then place a total of $k = \left\lfloor (\alpha_1/2)^{2/3} (\psi/\phi)^{2/3} / c' \right\rceil = 28$ transshipment nodes in the region following a contracted honeycomb configuration. If we were to double the size of the region, resulting in 200 square miles with 300 customers, we would obtain a solution consisting of 44 transshipment nodes placed in a contracted honeycomb configuration. If we were to increase the size of the region by a factor of 10, resulting in 1000 square miles with 1500 customers, our solution would have 131 transshipment nodes. This is simply a reflection of the basic property of the contracted honeycomb configuration that transshipment nodes are placed much more sparsely as one moves increasingly far from the central depot.

4 Asymptotic solutions to (1)

In this section, we analyze the solutions to problem (1) as the various coefficients become large or small relative to one another. Since we are only concerned with the limiting behavior of the model, we find it useful to express the utility functions in their highest-order terms. To this end, we assume that the service region R has a population t and we impose the following functional forms on $\mathrm{Fix}(\cdot)$, ϕ, and ψ:

- We assume that the fixed cost for $|X| = k$ hubs to serve the population t takes the form $\mathrm{Fix}(k; t) = k \cdot f(t/k)$, where $f(\tau)$ denotes the fixed cost associated with a single hub that provides service to a population of size τ. If we assume that the fixed costs follow an economy of scale, it is natural to assume that $f(\tau)$ is concave and increasing, and (since we are only concerned with the limiting behavior, i.e. the highest-order terms) we make the further assumption that $f(\tau) = a\tau^p$, where $0 \leq p \leq 1$. This is equivalent to assuming that the fixed costs follow the simplest possible Cobb-Douglas production function with increasing returns to scale [26].

- We assume that the backbone network cost for the hubs X to serve the population t takes the form $\phi_t\,\mathrm{BBN}(X)$, where $\mathrm{BBN}(\cdot)$ is of the form $\mathrm{Steiner}(\cdot)$, $\mathrm{MST}(\cdot)$, $\mathrm{TSP}(\cdot)$, $\mathrm{SN}(\cdot)$, $\mathrm{VRP}(\cdot)$, $\mathrm{CBG}(\cdot)$, or $\mathrm{CG}(\cdot)$, and ϕ_t is a concave increasing function of the population t. This models the case where a higher population results in higher backbone network costs (since there are more "things" to transport), but the network benefits from an economy of scale (see for example Section 3.1 of [11]). As in the fixed costs, we therefore assume that ϕ_t takes the form $\phi_t = bt^q$, where $0 \le q \le 1$.
- We assume that the local transportation costs take the form $t\,\mathrm{FW}(X,R)$. This simply says that the cost increases proportionally to the population in the region, which is justified by assuming that local transportation does not benefit from an economy of scale.

Our model in this section then takes the form

$$\underset{X}{\mathrm{minimize}}\; ka\,(t/k)^p + bt^q\,\mathrm{BBN}(X) + t\,\mathrm{FW}(X,R)\,. \tag{17}$$

We shall assume throughout this section that $\mathrm{Area}(R) = 1$ since we are considering the limiting behavior as $t \to \infty$. We now proceed to describe the optimal solution to (17) as $t \to \infty$ for the various forms of $\mathrm{BBN}(\cdot)$.

4.1 The case $b = 0$

Note first that if we do not impose backbone network costs, then by Section 2.1 it will suffice to consider the problem

$$\underset{k}{\mathrm{minimize}}\; ka\,(t/k)^p + t\alpha_1/\sqrt{k}$$

where $\alpha_1 \approx 0.37721$ as before, which is minimized at $k = ct^{\frac{2-2p}{3-2p}}$, where

$$c = \left[\frac{\alpha_1}{2a(1-p)}\right]^{\frac{2}{3-2p}}\,.$$

The optimal objective function value is then proportional to $t^{\frac{2-p}{3-2p}}$ (the proportionality constant can be computed, but we omit it here for brevity).

4.2 The case $\mathrm{BBN}(\cdot) \in \{\mathrm{Steiner}(\cdot), \mathrm{MST}(\cdot), \mathrm{TSP}(\cdot)\}$

Suppose that we adopt a Steiner tree, minimum spanning tree, or travelling salesman tour as our backbone network. We will show that the optimal solution to (17) depends on the relationship between p and $3/2 - 1/2q$:

- If $p > 3/2 - 1/2q$, then we claim that the uniform honeycomb heuristic, with $c = \left[\frac{\alpha_1}{2a(1-p)}\right]^{\frac{2}{3-2p}}$ and $k = ct^{\frac{2-2p}{3-2p}}$ as in Section 4.1, is asymptotically optimal as $t \to \infty$. Under a honeycomb configuration, we see that

$$\mathrm{MST}(X), \mathrm{TSP}(X) \sim \beta_0\sqrt{k} := \frac{\sqrt{6}}{3^{3/4}}\sqrt{k} \approx 1.0746\sqrt{k}$$

as explained in [5], and therefore that $\mathrm{Steiner}(X) \in \mathcal{O}(\sqrt{k})$ as well (this is because $1/2\,\mathrm{MST}(X) \le \mathrm{Steiner}(X) \le \mathrm{MST}(X)$; see for example [45]). Thus, objective function (17) is at most

$$ka\,(t/k)^p + bt^q \cdot \beta_0\sqrt{k} + t\alpha_1/\sqrt{k}\,. \tag{18}$$

We take the ratio of the fixed costs to the backbone network costs

$$\left.\frac{ka\,(t/k)^p}{bt^q \cdot \beta_0\sqrt{k}}\right|_{k=ct^{\frac{2-2p}{3-2p}}} \in \Omega\left(t^{\frac{1}{3-2p}-q}\right)$$

which is increasing in t provided that $p > 3/2 - {}^{1}/{}_{2q}$. This shows that as $t \to \infty$, the backbone network cost becomes arbitrarily small relative to the fixed costs, and therefore

$$\left.\frac{ka\,(t/k)^p + bt^q \cdot \beta_0\sqrt{k} + t\alpha_1/\sqrt{k}}{ka\,(t/k)^p + t\alpha_1/\sqrt{k}}\right|_{k=ct^{\frac{2-2p}{3-2p}}} \to 1$$

which proves asymptotic optimality, since the denominator in the above expression is clearly a lower bound on problem (17), given that it simply consists of neglecting the backbone network costs.

- If $p < 3/2 - {}^{1}/{}_{2q}$, then we claim that the Archimedes heuristic, with $k = t^{\frac{3-q-2p}{4-2p}}$ points placed equidistantly along an Archimedean spiral with length $\ell^* = t^{(1-q)/2}/(2\sqrt{b})$ (i.e. with polar equation $r = {}^{\theta}/{}_{2\pi\ell^*}$), is optimal as $t \to \infty$. First, we note that from Section 2.2, it is clear that an asymptotic lower bound for our problem is $\sqrt{b}t^{(q+1)/2}$; this is simply the optimal objective value $A\sqrt{\phi\psi}$ with $A = 1$, $\phi = bt^q$, and $\psi = t$ when fixed costs are ignored. When X consists of k points distributed along a spiral of length ℓ, then provided k is sufficiently large, we have

$$\mathrm{FW}(X, R) \le \frac{\ell}{4k} + \frac{1}{4\ell}$$

(this is true because the Voronoi diagram of X approximately consists of k rectangles having dimensions $\ell/k \times 1/\ell$, which is apparent from Figure 3b; the right-hand side of the above expression is the Fermat-Weber value of these under the ℓ_1 norm). Objective function (17) is then at most

$$\left. ka\,(t/k)^p + bt^q \cdot \ell^* + t\left(\frac{\ell}{4k} + \frac{1}{4\ell}\right)\right|_{k=t^{\frac{3-q-2p}{4-2p}},\,\ell^*=t^{(1-q)/2}/(2\sqrt{b})} = \sqrt{b}t^{(q+1)/2} + \mathcal{O}\left(t^{\frac{3+qp-q-p}{4-2p}}\right) \sim \sqrt{b}t^{(q+1)/2} \text{ as } t \to \infty$$

because $\frac{3+qp-q-p}{4-2p} < (q+1)/2$.

4.3 The case $\mathrm{BBN}(\cdot) = \mathrm{SN}(\cdot)$

Suppose that we adopt a star network topology as our backbone network. We will show that the optimal solution to (17) depends on the relationship between p and $\frac{3q}{2q+1}$:

- If $p > \frac{3q}{2q+1}$, then we claim that the uniform honeycomb heuristic, with $c = \left[\frac{\alpha_1}{2a(1-p)}\right]^{\frac{2}{3-2p}}$ and $k = ct^{\frac{2-2p}{3-2p}}$ as in Section 4.1, is asymptotically optimal as $t \to \infty$. Under this configuration, we can write (17) as

$$ka\,(t/k)^p + bt^q \cdot \beta k + t\alpha_1/\sqrt{k} \tag{19}$$

where $\beta = \mathrm{FW}(R)$ represents the average distance between a uniformly sampled point in R (or, for large k, a point in X) and $\bar{x}$, which we again assume to be the origin. We take the ratio of the fixed costs to the backbone network costs

$$\left.\frac{ka\,(t/k)^p}{bt^q \cdot \beta k}\right|_{k=ct^{\frac{2-2p}{3-2p}}} \in \Omega\left(t^{\frac{p}{3-2p}-q}\right)$$

which is increasing in t provided $p > \frac{3q}{2q+1}$. This shows that as $t \to \infty$, the backbone network cost becomes arbitrarily small relative to the fixed costs, and therefore

$$\left.\frac{ka\,(t/k)^p + bt^q \cdot \beta k + t\alpha_1/\sqrt{k}}{ka\,(t/k)^p + t\alpha_1/\sqrt{k}}\right|_{k=ct^{\frac{2-2p}{3-2p}}} \to 1$$

which proves asymptotic optimality, since the denominator in the above expression is clearly a lower bound on problem (17), given that it simply consists of neglecting the backbone network costs.

- Conversely, if $p < \frac{3q}{2q+1}$, then we claim that the "contracted honeycomb" configuration, with $c^{'} = \left(\iint_R \|x\|^{-2/3}\, dA\right)^{-1}$ and $k = (\alpha_1/2)^{2/3}(t/bt^q)^{2/3}/c^{'}$, is asymptotically optimal as $t \to \infty$. This is because, by (7), the backbone network costs approach
$$\left(\frac{\alpha_1}{2}\right)^{2/3}\left(\iint_R \|x\|^{1/3}\, dA\right)(bt^q)^{1/3}t^{2/3} \in \Omega\left(t^{(2+q)/3}\right),$$
whereas the fixed costs approach
$$ka\,(t/k)^p|_{k=(\alpha_1/2)^{2/3}(t/bt^q)^{2/3}/c'} \in \mathcal{O}\left(t^{(2-2q+p+2qp)/3}\right),$$
and thus we find that the backbone network costs dwarf the fixed costs as $t \to \infty$ since $(2+q)/3 > (2-2q+p+2qp)/3$.

4.4 The case $\mathrm{BBN}(\cdot) = \mathrm{VRP}(\cdot)$

Suppose that we adopt a capacitated VRP tour as our backbone network. As we have seen in Section 2.4, the backbone network costs incurred under such a topology are essentially inherited from either a star network or a TSP tour depending on the vehicle capacity κ. We will assume that $\kappa = \kappa_0 t^r$, i.e. that the vehicle capacities vary with respect to the population t; this simply models the case where different modes of transportation are available to provide service to the region as demand increases. Applying the result of Section 2.4 to our model (17), we find that the capacity constraints become increasingly restrictive when $r < (1-q)/2$, so that the star network approximation of $\mathrm{VRP}(\cdot)$ becomes tight as $t \to \infty$, and similarly the TSP tour approximation becomes tight when $r > (1-q)/2$. The optimal solution to (17) can then be classified as follows:

- If $r < (1-q)/2$, then our problem can be approximated as
$$\underset{X}{\text{minimize}}\; ka\,(t/k)^p + \frac{2b}{\kappa_0}t^{q-r}\,\mathrm{SN}(X) + t\,\mathrm{FW}(X,R)$$
as $t \to \infty$, and consequently the optimal solution depends on the relationship between p and $\frac{3(q-r)}{2(q-r)+1}$ (this is nothing more than a restatement of the result of Section 2.3, making the substitution $q \mapsto q-r$):
  - If $p > \frac{3(q-r)}{2(q-r)+1}$, then the uniform honeycomb heuristic is asymptotically optimal as $t \to \infty$ because the fixed costs dominate the backbone network costs.
  - If $p < \frac{3(q-r)}{2(q-r)+1}$, then the "contracted honeycomb" configuration is asymptotically optimal as $t \to \infty$ because the backbone network costs dominate the fixed costs.
- If $r > (1-q)/2$, then our problem can be approximated as
$$\underset{X}{\text{minimize}}\; ka\,(t/k)^p + bt^q\,\mathrm{TSP}(X) + t\,\mathrm{FW}(X,R)$$
as $t \to \infty$, and consequently the optimal solution depends on the relationship between p and $3/2 - 1/2q$ in the same fashion as in Section 4.2.

4.5 The case $\mathrm{BBN}(\cdot) = \mathrm{CBG}(\cdot)$

As we have seen previously in Section 2.5, the case where $\mathrm{BBN}(\cdot) = \mathrm{CBG}(\cdot)$ is a straightforward generalization of the case where $\mathrm{BBN}(\cdot) = \mathrm{SN}(\cdot)$. Thus, there is nothing more to do in this section because the result of Section 2.3 carries over without incident.

Backbone network	Conditions		Optimal configuration	k^*	Optimal objective value
Steiner/MST/TSP	$p > \frac{3}{2} - \frac{1}{2q}$		Honeycomb	$\propto t^{\frac{2-2p}{3-2p}}$	$\propto t^{\frac{2-p}{3-2p}}$
	$p < \frac{3}{2} - \frac{1}{2q}$		Archimedes	$\propto t^{\frac{3-2p-q}{4-2p}}$	$\propto t^{(q+1)/2}$
Star network/CBG	$p > \frac{3q}{2q+1}$		Honeycomb	$\propto t^{\frac{2-2p}{3-2p}}$	$\propto t^{\frac{2-p}{3-2p}}$
	$p < \frac{3q}{2q+1}$		Contracted honeycomb	$\propto t^{2(1-q)/3}$	$\propto t^{(q+2)/3}$
VRP	$r < (1-q)/2$	$p > \frac{3(q-r)}{2(q-r)+1}$	Honeycomb	$\propto t^{\frac{2-2p}{3-2p}}$	$\propto t^{\frac{2-p}{3-2p}}$
		$p < \frac{3(q-r)}{2(q-r)+1}$	Contracted honeycomb	$\propto t^{2[1-(q-r)]/3}$	$\propto t^{(q-r+2)/3}$
	$r > (1-q)/2$	$p > \frac{3}{2} - \frac{1}{2q}$	Honeycomb	$\propto t^{\frac{2-2p}{3-2p}}$	$\propto t^{\frac{2-p}{3-2p}}$
		$p < \frac{3}{2} - \frac{1}{2q}$	Archimedes	$\propto t^{\frac{3-2p-q}{4-2p}}$	$\propto t^{(q+1)/2}$
Complete graph	$p > \frac{3q+2}{2q+3}$		Honeycomb	$\propto t^{\frac{2-2p}{3-2p}}$	$\propto t^{\frac{2-p}{3-2p}}$
	$p < \frac{3q+2}{2q+3}$		Less contracted honeycomb	$\propto t^{2(1-q)/5}$	$\propto t^{(q+4)/5}$

Table 2: The optimal configurations, numbers of hubs, and objective values for various values of p and q and backbone network structures in (17).

4.6 The case $\mathrm{BBN}(\cdot) = \mathrm{CG}(\cdot)$

When we adopt a complete graph as the backbone network, we can follow precisely the same line of reasoning as in Section 4.3 to show that the optimal solution to (17) depends on the relationship between p and $\frac{3q+2}{2q+3}$:

- If $p > \frac{3q+2}{2q+3}$, the uniform honeycomb heuristic with with $c = \left[\frac{\alpha_1}{2a(1-p)}\right]^{\frac{2}{3-2p}}$ and $k = ct^{\frac{2-2p}{3-2p}}$ as in Section 4.1 gives an asymptotically optimal solution with objective value proportional to $t^{\frac{2-p}{3-2p}}$.
- If $p < \frac{3q+2}{2q+3}$, the "less contracted honeycomb" configuration, with $k = \frac{t^{2/5}}{c^{3/5}(bt^q)^{2/5}}$ and c, c', and c'' defined in (13), (14), and (15), is asymptotically optimal (within a factor of 15%) with objective value proportional to $t^{(q+4)/5}$.

4.7 Summary table and discussion

Table 2 and Figure 5 summarize the results of this section. Another interpretation of these results allows us to understand the benefits of improving infrastructures in either the fixed costs or the backbone network: for all seven backbone network topologies, the optimal configuration is either the honeycomb heuristic or a heuristic that is associated with that backbone network topology. One can also observe that, under the various conditions on p and q, it is always the case that either the fixed costs dominate the backbone network costs or that the backbone network costs dominate the fixed costs. Thus, for example, if we use a star network to connect our hubs and $p < \frac{3q}{2q+1}$, then there is little to be gained by reducing our fixed costs because they are already dwarfed by the backbone network costs as it is. Similarly, if we use a TSP tour as our backbone network and $p > 3/2 - 1/2q$, we gain little by cheapening our backbone network because the fixed costs are the dominant term. This allows us to quantify (in a very highly stylized sense, of course) the intrinsic trade-offs between such fixed costs and transportation costs as a function of the input parameters [43].

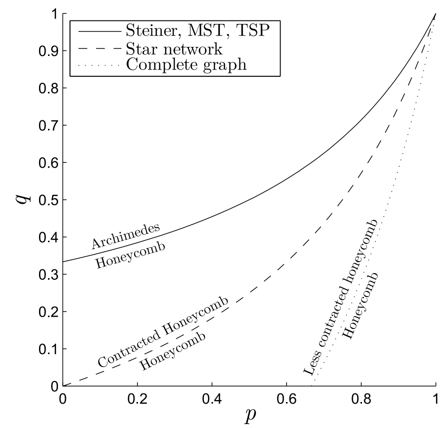

Figure 5: The boundary curves that distinguish different optimal solution configurations for various values of p and q in five of the backbone network structures (we have omitted the cases where $\mathrm{BBN}(\cdot) \in \{\mathrm{VRP}(\cdot), \mathrm{CBG}(\cdot)\}$ because they can be described in terms of the others). If the pair (p, q) lies above the curve associated with a particular backbone network configuration, then the backbone network costs dominate the fixed costs as $t \to \infty$. Conversely, if (p, q) lies below the curve of interest, then the fixed costs dominate the backbone network costs.

5 Multi-level networks

The problems we have considered thus far can be thought of as belonging to the class of *two-level* location and design problems: goods are first transported along the backbone network to facilities, then to the customers in the service region via direct trips. It is natural to generalize problem (1) to the case where we have multiple levels of distribution that occur between the facilities and the customers,

$$\underset{X^1,\ldots,X^n}{\text{minimize}} \sum_{i=1}^{n} \underset{i}{\mathrm{Fix}}(|X^i|) + \sum_{i=1}^{n} \phi_i \,\mathrm{BBN}_i(X^i) + \psi \,\mathrm{FW}(X^1, R)\,, \tag{20}$$

where X^i denotes the set of facilities at the ith "level"; note that it is only the lowest-level facilities X^1 that provide service to the customers in the region (which they do via direct trips). This setup is shown in Figure 6. In this section, we will consider the structure of the optimal solution to (20) when all backbone networks are star networks (which is also suggested in Figure 6). Thus, a facility $x_j^{i-1} \in X^{i-1}$ will be connected to the facility in X^i that is closest to it; let $\mathrm{NN}(X^i, X^{i-1})$ denote the "nearest neighbor" graph that is induced by this assumption. Since there are no facilities above the nth level, we simply assume that those facilities at the nth level are connected with a star network rooted at the geometric median of X^n, i.e. that $\mathrm{BBN}_n(X^n) = \mathrm{SN}(X^n)$. For simplicity, we will consider the case where no fixed costs are imposed on any of the facilities, i.e. $\mathrm{Fix}_i(\cdot) = 0$ for all levels. We devote the remainder of this section to a proof of the following theorem:

Theorem 9. *The optimal objective function value to the problem*

$$\underset{X^1,\ldots,X^n}{\text{minimize}}\, \phi_n \,\mathrm{SN}(X^n) + \sum_{i=1}^{n-1} \phi_i \,\mathrm{NN}(X^{i+1}, X^i) + \phi_0 \,\mathrm{FW}(X^1, R) \tag{21}$$

takes the form

$$\left(\frac{2^{n+1}-1}{2^{\frac{2+2^{n+1}(n-1)}{2^{n+1}-1}}}\right) \left(\prod_{i=0}^{n-1} a_i^{2^{n+1}-2^{n-i}}\right)^{\frac{1}{2^{n+1}-1}} \left(\prod_{i=0}^{n} \phi_i^{2^{n-i}}\right)^{\frac{1}{2^{n+1}-1}} \iint_R \|x\|^{\frac{1}{2^{n+1}-1}}\, dA \tag{22}$$

as $\phi_i/\phi_0 \to 0$ for all $i \geq 1$, where we define

$$a_i = \iint_{\mathrm{Hex}(1)} \|x\|^{\frac{1}{2^{i+1}-1}}\, dA$$

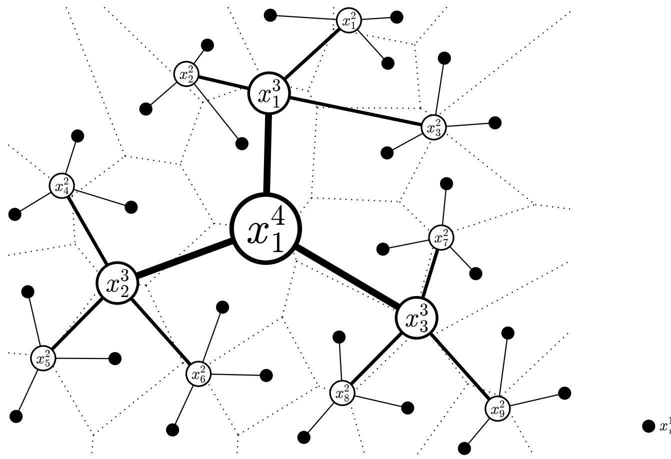

Figure 6: A four-stage hub-and-spoke network with star backbone networks at each level. For aesthetic purposes, we have refrained from labelling the first-level facilities $x_1^1, \ldots, x_k^1$. We also show the Voronoi partition induced by these first-level facilities as in Figure 1.

n	Optimal value to (21)
1	$\frac{3}{2^{2/3}}\left(a_0^2 a_1^3\right)^{1/3}\left(\phi_0^2\phi_1\right)^{1/3} A^{7/6}$
2	$\frac{7}{2^{10/7}}\left(a_0^4 a_1^6 a_2^7\right)^{1/7}\left(\phi_0^4\phi_1^2\phi_2\right)^{1/7} A^{15/14}$
3	$\frac{15}{2^{34/15}}\left(a_0^8 a_1^{12} a_2^{14} a_3^{15}\right)^{1/15}\left(\phi_0^8\phi_1^4\phi_2^2\phi_3\right)^{1/15} A^{31/30}$
4	$\frac{31}{2^{98/31}}\left(a_0^{16} a_1^{24} a_2^{28} a_3^{30} a_4^{31}\right)^{1/31}\left(\phi_0^{16}\phi_1^8\phi_2^4\phi_3^2\phi_4\right)^{1/31} A^{63/62}$

Table 3: Values of (23) for $n \in \{1, 2, 3, 4\}$.

with Hex(1) *denoting a regular hexagon with unit area, which simplifies to*

$$\left(\frac{2^{n+1}-1}{2^{\frac{2+2^{n+1}(n-1)}{2^{n+1}-1}}}\right)\left(\prod_{i=0}^{n} a_i^{2^{n+1}-2^{n-i}}\right)^{\frac{1}{2^{n+1}-1}}\left(\prod_{i=0}^{n}\phi_i^{2^{n-i}}\right)^{\frac{1}{2^{n+1}-1}} A^{\frac{2^{n+2}-1}{2^{n+2}-2}} \tag{23}$$

when R is a regular hexagon of area A. The optimal configuration of points at the nth level is a contracted honeycomb configuration that follows the distribution $f(x) = c\|x\|^{\frac{-2}{q+2}}$ for a suitable constant c, where $q = \frac{1}{2^n-1}$.

The above expression is quite unwieldy, but becomes clearer when we write out its first few values, which are shown in Table 3. Note that higher-level facilities are more concentrated about their centers than lower-level facilities because the exponent $\frac{-2}{q+2}$ approaches -1 from the right as n increases. We require a fairly simple lemma in order to prove this result:

Lemma 10. *Let R be a compact planar region with area A. As $\psi/\phi \to \infty$, the optimal objective value to the problem*

$$\underset{X}{\text{minimize}}\, \phi\, \mathrm{SN}(X) + \psi\, \mathrm{FW}_f(X, R)\,, \tag{24}$$

where $f(\tau) = \tau^q$ and $\mathrm{FW}_f(\cdot,\cdot)$ is as defined in Theorem 2, is given by

$$c\left(\phi^q\psi^2\right)^{\frac{1}{q+2}} \iint_R \|x\|^{\frac{q}{q+2}}\, dA\,,$$

where we define

$$c = \left(\frac{\alpha_q^2}{4q^q}\right)^{\frac{1}{q+2}} (q+2)$$

and

$$\alpha_q = \iint_{\mathrm{Hex}(1)} \|x\|^q \, dA \, .$$

Proof. Note that this is a generalization of Section 2.3 (which deals with the special case $q = 1$) and that our values α_q generalize our previous definition of α_1. This result is proven in an entirely analogous manner to Section 2.3. □

Remark 11. If we vary the area A but retain the same shape, the integral $\iint_R \|x\|^{\frac{q}{q+2}} \, dA$ in the above scales proportionally to $A^{\frac{3q+4}{2q+4}}$.

We can now proceed to prove Theorem 9 by induction:

Proof of Theorem 9. It is clearly true that Theorem 9 holds for the base case where $n = 1$, which was demonstrated in Section 2.3. Assume that Theorem 9 holds for networks of up to $n-1$ levels and consider the problem with n levels; for any placement of the points $X^n = \{x_1^n, \ldots, x_k^n\}$ (with k obviously a variable) let V_j denote the Voronoi cell of point x_j^n. By the induction hypothesis, we see that the optimal cost to cover cell V_j with those facilities at levels 1 through $n-1$ is given by

$$\left(\frac{2^n - 1}{2^{\frac{2+2^n(n-2)}{2^n-1}}}\right) \left(\prod_{i=0}^{n-2} a_i^{2^n - 2^{n-1-i}}\right)^{\frac{1}{2^n-1}} \left(\prod_{i=0}^{n-1} \phi_i^{2^{n-1-i}}\right)^{\frac{1}{2^n-1}} \iint_{V_j} \|x - x_j^n\|^{\frac{1}{2^n-1}} \, dA$$

and therefore the total cost of coverage of these regions is simply the sum of this over all cells:

$$\begin{aligned}
\sum_{i=1}^{n-1} \phi_i \, \mathrm{NN}(X^{i+1}, X^i) + \phi_0 \, \mathrm{FW}(X^1, R) \quad &\sim \quad \left(\frac{2^n - 1}{2^{\frac{2+2^n(n-2)}{2^n-1}}}\right) \left(\prod_{i=0}^{n-2} a_i^{2^n - 2^{n-1-i}}\right)^{\frac{1}{2^n-1}} \left(\prod_{i=0}^{n-1} \phi_i^{2^{n-1-i}}\right)^{\frac{1}{2^n-1}} \sum_{j=1}^{k} \iint_{V_j} \|x - x_j^n\|^{\frac{1}{2^n-1}} \, dA \\
&= \quad \underbrace{\left(\frac{2^n - 1}{2^{\frac{2+2^n(n-2)}{2^n-1}}}\right) \left(\prod_{i=0}^{n-2} a_i^{2^n - 2^{n-1-i}}\right)^{\frac{1}{2^n-1}} \left(\prod_{i=0}^{n-1} \phi_i^{2^{n-1-i}}\right)^{\frac{1}{2^n-1}}}_{\psi} \mathrm{FW}_f(X^n, R)
\end{aligned}$$

where $f(\tau) = \tau^{\frac{1}{2^n-1}}$. We therefore find that problem (21) can be written as

$$\underset{X^n}{\text{minimize}} \, \phi_n \, \mathrm{SN}(X^n) + \psi \, \mathrm{FW}_f(X^n, R) \, ,$$

whose optimal objective value is given by Lemma 10; the remainder of the proof then becomes a tedious calculation by substituting for ψ which we omit for brevity. □

To conclude this section, Figure 7 shows an optimal configuration of a three-level network.

Part II

Algorithmic analysis

6 An algorithmic formulation of (1)

In this section we describe an algorithm for minimizing objective function (1) within a constant factor. Unlike the preceding analysis in Part I, we will require upper and lower bounds for (1) that are *uniform*: that is, we must find bounds that are valid for all possible input parameters, rather than merely looking at limiting behaviors as we did before. This complicates

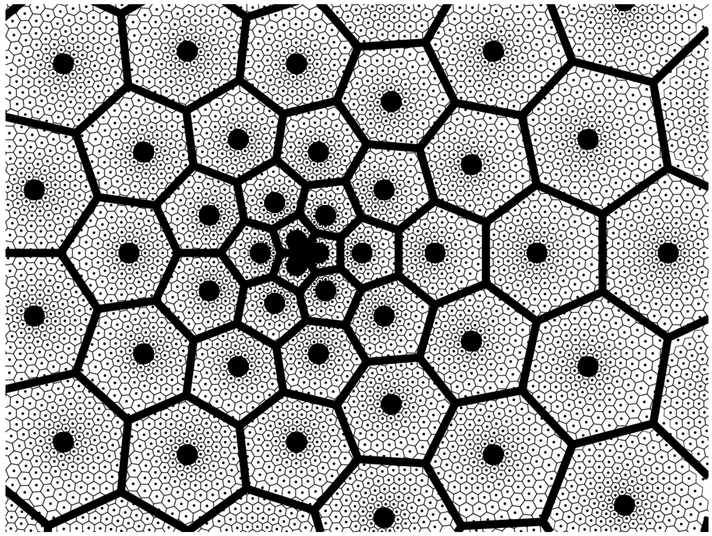

Figure 7: An optimal configuration for a three-level network.

matters because we have to explicitly take shape constraints of the input region into account, and as a consequence, the bounds we derive are somewhat unwieldy.

We will assume without loss of generality that $\psi = 1$, and for purposes of clarity we will treat the fixed costs as a hard constraint that $|X| \leq k_0$ for some fixed input k_0. We will also assume that the service region R is a convex polygon C and that C is oriented in such a way that $\operatorname{diam}(C)$ is aligned with the x-axis, so that C is contained in a box of dimensions $(w = \operatorname{diam}(C)) \times h$. We will further assume without loss of generality that $w = 1/h$, which implies by convexity of C that $1/2 \leq A = \operatorname{Area}(C) \leq 1$. For purposes of clarity, we will use the terms w and $1/h$ interchangeably depending on the context. In summary, we will show how to obtain an approximately optimal solution for the problem

$$\begin{array}{rcl} \underset{X}{\text{minimize}}\, F(X) = \phi\, \mathrm{BBN}(X) + \mathrm{FW}(X, C) & & s.t. \\ |X| & \leq & k_0 \end{array} \tag{25}$$

for a given convex polygon C, a backbone network topology $\mathrm{BBN}(\cdot)$, a positive scalar ϕ, and a positive integer k_0. Our general procedure will be to run a simple subroutine, ApproxFW (which is itself based on an even simpler subroutine, RectanglePartition), on C, applying several "strategic" choices of $k = |X|$. These are described in Algorithms 1 and 2 and Figures 8 and 9. As an aside, it turns out that Algorithm 2 is a constant-factor approximation algorithm for the continuous Fermat-Weber problem in a convex polygon (that is, minimizing $\mathrm{FW}(X, C)$ in a given convex polygon C with a constraint that $|X| = k_0$), with approximation constant 2.74 [9].

In order to simplify our exposition as much as possible, we will apply a rigorous analysis only to the case where $\mathrm{BBN}(\cdot) = \mathrm{SN}(\cdot)$. This is because the case where $\mathrm{BBN}(\cdot) = \mathrm{TSP}(\cdot)$ was already considered in [8], and the analysis therein can be extended to the cases $\mathrm{BBN}(\cdot) = \mathrm{Steiner}(\cdot)$ and $\mathrm{BBN}(\cdot) = \mathrm{MST}(\cdot)$ in a straightforward way. Our analysis here also suggests a natural approach for the case where $\mathrm{BBN}(\cdot) = \mathrm{CG}(\cdot)$ because for any point set X we have already seen that $^{k}\!/_{2}\, \mathrm{SN}(X) \leq \mathrm{CG}(X) \leq k\, \mathrm{SN}(X)$. The key idea is to derive *uniform* bounds that relate $\mathrm{BBN}(X)$ and $\mathrm{FW}(X, C)$ in a convex polygon, as we will do in Theorems 12, 15, and 17, for example, which relate $\mathrm{SN}(X)$ and $\mathrm{FW}(X)$. One would similarly use the same bounds to relate $k\, \mathrm{SN}(X)$ and $\mathrm{FW}(X)$ to derive an approximation analysis for the case where $\mathrm{BBN}(\cdot) = \mathrm{CG}(\cdot)$. We will list all of the approximation constants associated with these five backbone network topologies in Table 4; we will disregard the cases where $\mathrm{BBN}(\cdot) = \mathrm{VRP}(\cdot)$ and $\mathrm{BBN}(\cdot) = \mathrm{CBG}(\cdot)$ because they require additional input parameters, namely the vehicle capacities and the facilities Y.

Input: An axis-aligned rectangle R and an integer k.
Output: A partition of R into k rectangles, each having area $\mathrm{Area}(R)/k$.
if $k = 1$ **then**
    return R;
else
    Set $k_1 = \lfloor k/2 \rfloor$ and $k_2 = \lceil k/2 \rceil$;
    Let w denote the width of R and h the height; **if** $w \geq h$ **then**
        With a vertical line, divide R into two pieces R_1 and R_2 with area $\frac{k_1}{k} \cdot \mathrm{Area}(R)$ on the right and $\frac{k_2}{k} \cdot \mathrm{Area}(R)$ on the left;
    else
        With a horizontal line, divide R into two pieces R_1 and R_2 with area $\frac{k_1}{k} \cdot \mathrm{Area}(R)$ on the top and $\frac{k_2}{k} \cdot \mathrm{Area}(R)$ on the bottom;
    end
    return $\mathit{RectanglePartition}(R_1, k_1) \cup \mathit{RectanglePartition}(R_2, k_2)$;
end

Algorithm 1: Algorithm RectanglePartition(R, k) takes as input an axis-aligned rectangle R and a positive integer k. This is used as a subroutine in Algorithm 2.

Input: A convex polygon C and an integer k.
Output: The locations of k points x_i in C that approximately minimize $\mathrm{FW}(C, k)$ within a factor of 2.74.
Align a diameter of C with the coordinate x-axis;
Let $\square C$ denote an axis-aligned box of dimensions $w \times h$, where $w = \mathrm{diam}(C)$;
Let $R_1, \ldots, R_k = \mathrm{RectanglePartition}(\square C, k)$;
for $i \in \{1, \ldots, k\}$ **do**
    Let c_i denote the center of R_i;
    if $c_i \in C$ **then**
        Set $x_i = c_i$;
    else
        Set x_i to be the projection of c_i on C;
    end
end
return $x_1, \ldots, x_k$;

Algorithm 2: Algorithm ApproxFW(C, k) takes as input a convex polygon C and an integer k. This is used as a subroutine in Algorithm 3.

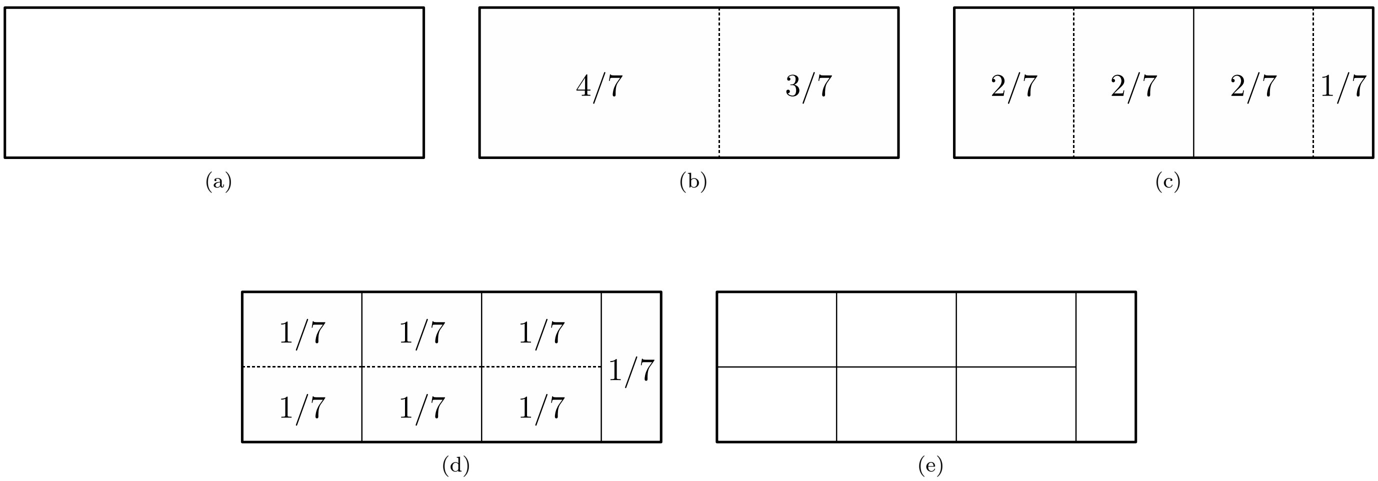

Figure 8: The input and output of Algorithm 1. We begin in (8a) with a rectangle R and an integer $k = 7$; here we assume that $\text{Area}(R) = 1$. In Figures (8b) through (8d), we subdivide R into smaller rectangles by a recursive subdivision; the areas of each sub-rectangle are shown. Figure (8e) shows the output.

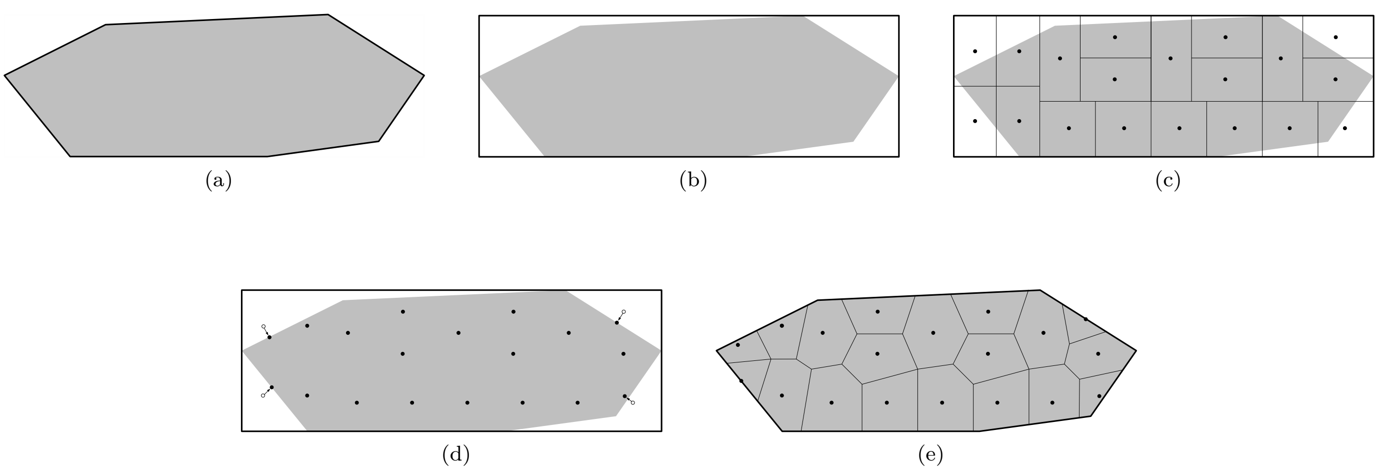

Figure 9: The input and output of Algorithm 2. We begin in (9a) with a convex polygon C, whose axis-aligned bounding box $\square C$ is computed in (9b). The bounding box is then partitioned into $k = 19$ equal-area pieces in (9c) using Algorithm 1. Some of the centers of these pieces are then relocated in (9d), and (9e) shows the output and Voronoi partition.

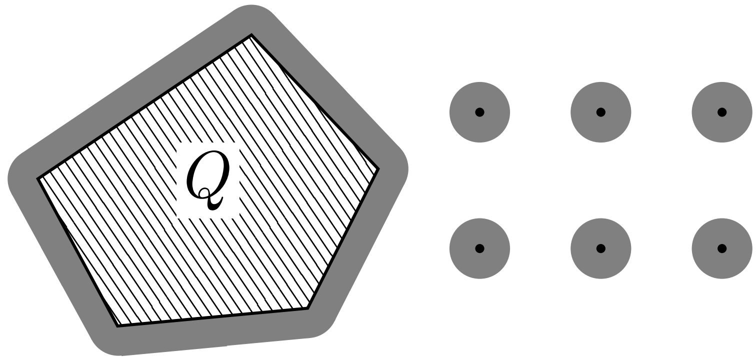

Figure 10: The optimal region R that minimizes $\mathrm{FW}(X^{'} \cup Q, R)$ in gray, where $k^{'} = |X^{'}| = 6$.

6.1 Lower bounds

In this section we introduce some lower bounding functions that we will use in proving that our proposed Algorithm 3 minimizes (25) within a constant factor.

6.1.1 Lower bounds for $\mathrm{BBN}(\cdot) = \mathrm{SN}(\cdot)$

When we adopt a star network as our backbone network topology, we find three useful lower bounds which follow below.

Theorem 12. *Suppose that $X = \{x_1, \ldots, x_k\}$ is a set of points in a convex polygon C with area A. Then*

$$\phi\,\mathrm{SN}(X) + \mathrm{FW}(X, C) \geq \phi k^{'} \sqrt{\frac{Ap}{\pi}} + \frac{A^{3/2}}{3\sqrt{\pi}} \cdot \frac{\left(\sqrt{p(k^{'}+1) - k^{'}p^2} - p\right)^2 \left(p + 2\sqrt{p(k^{'}+1) - k^{'}p^2}\right)}{(k^{'}+1)^2\, p^{3/2}}\,, \tag{26}$$

with $p = 1/7$ and

$$k^{'} = \max\left\{0\,,\; \frac{2 \cdot 21^{1/3}}{21}\left(\frac{3A^{2/3}}{\phi^{2/3}} - \frac{A^{1/3}}{\phi^{1/3}}\right) - 1\right\}\,.$$

Proof. Suppose without loss of generality that $\bar{x}$ is the origin. Consider a ball B_r about the origin with radius r. Consider the lower bound for $\mathrm{SN}(X)$ defined by

$$\mathrm{SNLB}_r(X) = \sum_{i=1}^{|X|} \begin{cases} 0 & \text{if } ||x_i|| \leq r \\ r & \text{otherwise.} \end{cases}$$

We can consider the related problem of minimizing $\phi\,\mathrm{SNLB}_r(X) + \mathrm{FW}(X, C)$, or equivalently

$$\phi r |X \setminus B_r| + \mathrm{FW}(X, C \setminus B_r)\,,$$

since we can place infinitely many elements of X inside B_r without incurring any additional penalty on the backbone network. We now attempt to find a lower bound for $\mathrm{FW}(X, C \setminus B_r)$, and to this end we require the following lemma:

Lemma 13. *Suppose that Q is a convex region in the plane with boundary length $\ell^{'}$ and that $X^{'} = \{x_1, \ldots, x_{k^{'}}\}$ is a finite set of points in the plane. Then for any region R outside of Q with area $A^{'}$, we have*

$$\mathrm{FW}(X^{'} \cup Q, R) \geq \frac{\left(\sqrt{\ell^{'2} + 4A^{'}\pi(k^{'}+1)} - \ell^{'}\right)^2 \left(2\sqrt{\ell^{'2} + 4A^{'}\pi(k^{'}+1)} + \ell^{'}\right)}{24\pi^2(k^{'}+1)^2} \tag{27}$$

where we define

$$\mathrm{FW}(X^{'} \cup Q, R) = \iint_R \min\left\{d(x, Q), \min_{i \in \{1, \ldots, k^{'}\}} ||x - x_i||\right\} dA\,.$$

Proof. It is clear that if Q is convex then $\text{Area}(N_\epsilon(Q)) = \epsilon\ell^{'} + \pi\epsilon^2$ for all ϵ. It is also clear that the region R that minimizes $\text{FW}(X^{'} \cup Q, R)$ is precisely given by $N_\epsilon(Q \cup X^{'})$ for an appropriate choice of ϵ such that $\text{Area}(N_\epsilon(X^{'} \cup Q)) = A^{'}$; see Figure 10. It follows that we should solve

$$(\epsilon\ell^{'} + \pi\epsilon^2) + k^{'}\pi\epsilon^2 = A^{'}$$

for ϵ, which gives

$$\epsilon = \frac{\sqrt{\ell'^2 + 4A'\pi(k'+1)} - \ell^{'}}{2\pi(k'+1)}\,.$$

The minimal Fermat-Weber value is attained when R is the disjoint union of $k^{'}$ balls of radius ϵ about the points x_i plus the neighborhood $N_\epsilon(Q)$, as shown in Figure 10. Their Fermat-Weber value is precisely the right-hand side of (27). $\square$

We now continue with the proof of Theorem 12. It is straightforward to verify algebraically that the right-hand side of (27) is decreasing in $\ell^{'}$ because for any non-negative constant c,

$$\frac{\partial}{\partial\ell'}\left(\sqrt{\ell'^2+c} - \ell^{'}\right)^2\left(2\sqrt{\ell'^2+c} + \ell^{'}\right) = 6\ell^{'}\sqrt{\ell'^2+c} - 6\ell^{'2} - 3c \le 0\,.$$

Having established the preceding result, we let p denote the fraction of area of C that is contained in B_r, so that $\text{Area}(C \cap B_R) = Ap$ and $\text{Area}(C \setminus B_r) = A(1-p)$. In Section B of the Online Supplement, we show that that $\text{length}((\partial B_r) \cap C) \le 2\sqrt{\pi Ap}$. Applying Lemma 13 with $Q = B_r$, $A^{'} = A(1-p)$ and $\ell^{'} = 2\sqrt{\pi Ap}$, we find that

$$\text{FW}(X \cup B_r, C \setminus B_r) \ge \frac{A^{3/2}}{3\sqrt{\pi}} \cdot \frac{\left(\sqrt{p(k'+1) - k'p^2} - p\right)^2\left(p + 2\sqrt{p(k'+1) - k'p^2}\right)}{(k'+1)^2\,p^{3/2}}$$

where $k^{'} = |X \setminus B_r|$ as before, and, using the fact that $r \ge \sqrt{Ap/\pi}$, we find that for any point set X,

$$\phi\,\text{SN}(X) + \text{FW}(X, C) \ge \phi k^{'}\sqrt{\frac{Ap}{\pi}} + \frac{A^{3/2}}{3\sqrt{\pi}} \cdot \frac{\left(\sqrt{p(k'+1) - k'p^2} - p\right)^2\left(p + 2\sqrt{p(k'+1) - kp^2}\right)}{(k'+1)^2\,p^{3/2}}\,.$$

In order to remove the dependency of the right-hand side on X (since $k^{'} = |X \setminus B_r|$ depends on X), we are free to simply take a minimum over all values of $k^{'}$:

$$\phi\,\text{SN}(X) + \text{FW}(X, C) \ge \min_{k' \ge 0}\left\{\phi k^{'}\sqrt{\frac{Ap}{\pi}} + \frac{A^{3/2}}{3\sqrt{\pi}} \cdot \frac{\left(\sqrt{p(k'+1) - k'p^2} - p\right)^2\left(p + 2\sqrt{p(k'+1) - kp^2}\right)}{(k'+1)^2\,p^{3/2}}\right\}\,.$$

In order to determine a closed-form lower bound for the left-hand side $\phi\,\text{SN}(X) + \text{FW}(X, C)$, it would be sensible to differentiate the argument within the $\min_{k'}\{\cdot\}$ with respect to $k^{'}$, set the result to zero, then solve for $k^{'}$. Before doing so, we note that the above inequality holds for any value of p whatsoever, and therefore we are free to simply fix $p = 1/7$ (for reasons explained in Remark 14). The differentiation and solution for $k^{'}$ is then performed, which gives

$$\begin{aligned}&\arg\min_{k' \ge 0}\left\{\phi k^{'}\sqrt{\frac{Ap}{\pi}} + \frac{A^{3/2}}{3\sqrt{\pi}} \cdot \frac{\left(\sqrt{p(k'+1) - k'p^2} - p\right)^2\left(p + 2\sqrt{p(k'+1) - kp^2}\right)}{(k'+1)^2\,p^{3/2}}\right\}\\ = \quad &\max\left\{0\,,\ \frac{2 \cdot 21^{1/3}}{21}\left(\frac{3A^{2/3}}{\phi^{2/3}} - \frac{A^{1/3}}{\phi^{1/3}}\right) - 1\right\}\,,\end{aligned}$$

thus completing the proof. $\square$

Remark 14. The selection $p = 1/7$ in the above proof is not arbitrary; our reasoning follows thusly: as $\phi \to 0$, the backbone network costs are cheaper, and therefore it is in our interests to place more points in $C \setminus B_r$, i.e. to increase $k^{'}$. When $k^{'}$ is large, we see that

$$\phi k^{'} \sqrt{\frac{Ap}{\pi}} + \frac{A^{3/2}}{3\sqrt{\pi}} \cdot \frac{\left(\sqrt{p(k'+1) - k'p^2} - p\right)^2 \left(p + 2\sqrt{p(k'+1) - kp^2}\right)}{(k'+1)^2\, p^{3/2}} \sim \phi k^{'} \sqrt{\frac{Ap}{\pi}} + \frac{2A^{3/2}}{3\sqrt{\pi}} \cdot \frac{(1-p)^{3/2}}{\sqrt{k'}}\,.$$

The right-hand side of the above is minimized at

$$k^{'} = \frac{1}{3^{2/3}} \cdot \frac{A^{2/3}(1-p)}{p^{1/3}\phi^{2/3}}\,,$$

at which point we find that

$$\phi k^{'} \sqrt{\frac{Ap}{\pi}} + \frac{2A^{3/2}}{3\sqrt{\pi}} \cdot \frac{(1-p)^{3/2}}{\sqrt{k'}} = \frac{\phi^{1/3} 3^{1/3} A^{7/6} p^{1/6} (1-p)}{\sqrt{\pi}}$$

which is maximized at $p = 1/7$ (it is in our interests to select a value of p that maximizes the above expression because we want our lower bound to be as tight as possible). By this very reasoning, we also find that as $\phi \to 0$, the lower bound satisfies

$$\phi k^{'} \sqrt{\frac{Ap}{\pi}} + \frac{A^{3/2}}{3\sqrt{\pi}} \cdot \frac{\left(\sqrt{p(k'+1) - k'p^2} - p\right)^2 \left(p + 2\sqrt{p(k'+1) - k'p^2}\right)}{(k'+1)^2\, p^{3/2}} \sim \frac{6 \cdot \sqrt{7} \cdot 21^{1/3} A^{7/6}}{49\sqrt{\pi}} \cdot \phi^{1/3}\,.$$

This proportionality to $A^{7/6}\phi^{1/3}$ was also present in our asymptotic analysis in Section 2.3; the difference is that the bound derived in Theorem 12 holds for any input parameters whereas the result of Theorem 5 holds only in the limiting case where $\phi/\psi \to 0$.

The next two bounds in Theorems 15 and 17 are useful when the input polygon C is "skinny" or when ϕ/ψ is large; as such, they do not have a counterpart in the asymptotic result of Part I of this paper.

Theorem 15. *Suppose that $X = \{x_1, \ldots, x_k\}$ is a set of points in a convex polygon C with area A, which is itself contained in a minimum bounding box $\square C$ of dimensions $w \times h$. Then*

$$\phi\, \mathrm{SN}(X) + \psi\, \mathrm{FW}(X, C) \geq \phi k^{'} \cdot \frac{Ap}{2h} + \frac{\left(\sqrt{16h^2 + 4A(1-p)\pi(k'+1)} - 4h\right)^2 \left(2\sqrt{16h^2 + 4A(1-p)\pi(k'+1)} + 4h\right)}{24\pi^2 (k'+1)^2}\,, \tag{28}$$

where $p = 1/4$ and

$$k^{'} = \max\left\{0\,,\ \frac{3^{1/3}A^{1/3}}{\pi^{1/3}} \cdot \frac{h^{2/3}}{\phi^{2/3}} - \frac{8 \cdot 3^{2/3}}{3\pi^{2/3}A^{1/3}} \cdot \frac{h^{4/3}}{\phi^{1/3}} - 1\right\}\,.$$

Proof. See Section C of the Online Supplement. ☐

Remark 16. Using the same reasoning as in Remark 14, we can show that, as $\max\{\phi, h\} \to 0$, the lower bound satisfies

$$\phi k^{'} \cdot \frac{Ap}{2h} + \frac{\left(\sqrt{16h^2 + 4A(1-p)\pi(k'+1)} - 4h\right)^2 \left(2\sqrt{16h^2 + 4A(1-p)\pi(k'+1)} + 4h\right)}{24\pi^2 (k'+1)^2} \sim \frac{3^{4/3}A^{4/3}}{8\pi^{1/3}} \cdot \frac{\phi^{1/3}}{h^{1/3}} - \frac{A}{8} \cdot \frac{\phi}{h}\,.$$

Theorem 17. *Suppose that $X = \{x_1, \ldots, x_k\}$ is a set of points in a convex polygon C with area A, which is itself contained in a minimum bounding box $\square C$ of dimensions $w \times h$. Then for any $p \in (0, 1)$, we have*

$$\phi\, \mathrm{SN}(X) + \mathrm{FW}(X, C) \geq \phi k^{'} \cdot \frac{Ap}{2h} + \frac{A^2(1-p)^2}{4h(k'+1)}$$

where

$$k^{'} = \max\left\{\frac{\sqrt{A}(1-p)}{\sqrt{2p\phi}} - 1\,,\ 0\right\}\,. \tag{29}$$

Proof. See Section D of the Online Supplement. ☐

Remark 18. Substituting $k^{'}$, the lower bound can be expressed equivalently as

$$\phi k^{'} \cdot \frac{Ap}{2h} + \frac{A^2(1-p)^2}{4h(k'+1)} = \frac{(2A)^{3/2}(1-p)\sqrt{p\phi} - 2Ap\phi}{4h} \,.$$

6.2 Upper bounds

We begin this section by defining a function $H(A, w, h)$, which we will use in all of the forthcoming backbone network topologies, which is an upper bound on the Fermat-Weber value of a convex region with area A contained in a box of dimensions $w \times h$:

Theorem 19. *Suppose that C is a convex region with area A in a rectangle R having dimensions $w \times h$, with $w \geq h$. We have*

$$\mathrm{FW}(C) \leq H(A,w,h) := \begin{cases} \left[\log\left(\frac{h+\sqrt{w^2+h^2}}{wa+w\sqrt{1+a^2}}\right) - a\sqrt{1+a^2}\right]\frac{w^3}{12} + \left[\log\left(\frac{bw+b\sqrt{w^2+h^2}}{h+h\sqrt{b^2+1}}\right) - \frac{\sqrt{b^2+1}}{b^2}\right]\frac{h^3}{12} + \frac{wh\sqrt{w^2+h^2}}{6} & \text{if } A < wh - \frac{h}{2}\sqrt{w^2-h^2} \\ \log\left(\frac{h+\sqrt{w^2+h^2}}{w}\right)\cdot\frac{w^3}{12} + \left[\log\left(\frac{cw+c\sqrt{w^2+h^2}}{h+h\sqrt{c^2+1}}\right) - \frac{\sqrt{1+c^2}}{c^2}\right]\frac{h^3}{12} + \frac{1}{6}wh\sqrt{w^2+h^2} & \text{otherwise}\,, \end{cases}$$

where

$$\begin{aligned} a &= \frac{w^3h - wh^3 - 2(wh-A)\sqrt{(w^2+h^2)^2 - 8hwA + 4A^2}}{2Awh - 2w^2h^2 - w^2\sqrt{(w^2+h^2)^2 - 8hwA + 4A^2}} \\ b &= \frac{2(wh^3 - Ah^2) + wh\sqrt{h^4 + 2w^2h^2 + w^4 - 8Awh + 4A^2}}{w^4 + 3w^2h^2 - 8Awh + 4A^2} \\ c &= \frac{h^2}{2(wh-A)}\,. \end{aligned}$$

Proof. See Section E of the Online Supplement. ☐

Remark 20. It is not hard to show that, if we fix the product wh, then as $h/w \to 0$, we have

$$H(A,w,h) \sim \frac{2}{3}Aw - \frac{1}{12}w^2h - \frac{1}{3}\cdot\frac{A^2}{h} \tag{30}$$

for all A (see the end of Section E of the Online Supplement). It can also be shown that, for fixed w and h, the function $H(A, w, h)$ is concave in A, and that the function $H(A, 1/h, h)$ is decreasing in h whenever $h \leq 1$.

Definition 21. The *aspect ratio* of a rectangle R, written $\mathrm{AR}(R)$, is the ratio of the longer side of R to the shorter side.

Before defining the appropriate values of k that should be passed to Algorithm 2 to solve problem (25), we find it useful to state four claims regarding Algorithms 1 and 2 which are easy to verify:

Claim 22. Suppose that R is a box of dimensions $w \times h$, where $w \geq h$, and that $\{R_1, \ldots, R_k\} = \mathsf{RectanglePartition}(R, k)$ is the output of Algorithm 1. If $k \geq w/3h$, then we have $\mathrm{AR}(R_i) \leq 3$ for all sub-rectangles R_i. If $k < w/3h$, then $\mathrm{AR}(R_i) = w/hk$ for all R_i.

Proof. See Section F of the Online Supplement. ☐

Claim 23. Suppose that R is a box of dimensions $w \times h$, where $w \geq h$, and that $\{R_1, \ldots, R_k\} = \mathsf{RectanglePartition}(R, k)$ is the output of Algorithm 1. If $k \leq 2w/h$, then all sub-rectangles R_i are identical, with width w/k and height h. $\mathrm{BBN}(\cdot) \in \{\mathrm{Steiner}(\cdot), \mathrm{MST}(\cdot), \mathrm{TSP}(\cdot), \mathrm{SN}(\cdot), \mathrm{CG}(\cdot)\}$

Proof. Obvious by inspection. ☐

Claim 24. Suppose that C is a convex polygon and $\{R_1, \dots, R_k\} = \mathsf{RectanglePartition}(\square C, k)$ is the output of Algorithm 1 applied to $\square C$. Further suppose that $\{c_1, \dots, c_k\}$ is the set of centers of the rectangles $\{R_1, \dots, R_k\}$ and that $\{x_1, \dots, x_k\} = \mathsf{ApproxFW}(C, k)$ is the output of Algorithm 2. Then $\mathrm{FW}(\{c_1, \dots, c_k\}, C) \geq \mathrm{FW}(\{x_1, \dots, x_k\}, C)$ and $\mathrm{BBN}(\{c_1, \dots, c_k\}) \geq \mathrm{BBN}(\{x_1, \dots, x_k\})$ for any of the five backbone network configurations under consideration.

Proof. It is clear from Algorithm 2 that we only have $c_i \neq x_i$ if $c_i \notin C$, so that x_i is the *projection* of c_i on C. It is a well-known fact [48] of convex analysis that projection operators onto closed convex sets are *nonexpansive*, i.e. that if $P_C(x)$ denotes the projection of x onto a convex set C, then $||x - y|| \geq ||P_C(x) - P_C(y)||$. The above claim immediately follows from this fact. $\square$

Claim 24 is helpful to us because it allows us to assume, in our upper bounding analysis below, that $p_i = c_i$ for all $i \in \{1, \dots, k\}$, because the case where $c_i \neq p_i$ leads to our using a projection operator which can only *decrease* our objective function (25).

Claim 25. Suppose that C is a convex polygon whose bounding box has dimensions $(w = 1/h) \times h$, where $w \geq h$, and that $\{x_1, \dots, x_k\} = \mathsf{ApproxFW}(C, k)$ is the output of Algorithm 2. Then if $k \geq {}^{w}\!/_{3h}$, we have $\mathrm{FW}(X, C) \leq \alpha/\sqrt{k}$, where $\alpha = H(A, \sqrt{3}, 1/\sqrt{3})$.

Proof. As in Claim 22, we know that the sub-rectangles R_i that led to the points x_i all have an aspect ratio of at most 3, and therefore the maximum value of $\mathrm{FW}(X, C)$ is attained when each of the rectangles has an aspect ratio of exactly 3 and contains area A/k (here we are using concavity of $H(\cdot)$ in its first argument which we observed in Remark 20). Thus, $\mathrm{FW}(X, C)$ is bounded above by $k \cdot H(A/k, \sqrt{3/k}, 1/\sqrt{3k}) = k \cdot (H(A, \sqrt{3}, 1/\sqrt{3})/k^{3/2}) = \alpha/\sqrt{k}$. $\square$

Using the preceding results we can now present our approximation algorithm $\mathsf{HubPlacement}$ for placing hubs so as to minimize (25), which is given in Algorithm 3. Note that Algorithm 3 simply consists of an iterated application of

Input: A convex polygon C with area $A \in [1/2, 1]$ contained in a minimum bounding box of dimensions $(\mathrm{diam}(C) = 1/h = w) \times h$, a backbone network topology $\mathrm{BBN}(\cdot) \in \{\mathrm{Steiner}(\cdot), \mathrm{MST}(\cdot), \mathrm{TSP}(\cdot), \mathrm{SN}(\cdot), \mathrm{CG}(\cdot)\}$, a positive scalar ϕ, and a positive integer k_0.
Output: The locations of a set of points X^* in C that approximately minimize, within a constant factor, the objective function

$$F(X) = \phi\, \mathrm{BBN}(X) + \mathrm{FW}(X, C)\,,$$

subject to the constraint that $|X| \leq k_0$.

Let $\alpha = H(A, \sqrt{3}, 1/\sqrt{3})$;
if $\mathrm{BBN}(\cdot) \in \{\mathrm{Steiner}(\cdot), \mathrm{MST}(\cdot), \mathrm{TSP}(\cdot)\}$ **then**
  Set $K = \{1, \lfloor w/h \rceil, \lfloor {}^{\alpha}\!/_{2\phi} \rceil, \lfloor {}^{\alpha}\!/_{\sqrt{3}\phi} \rceil, k_0\}$;
else if $\mathrm{BBN}(\cdot) \in \mathrm{SN}(\cdot)$ **then**
  Set $K = \left\{1, \left\lfloor \sqrt{\frac{8A - 4A^2 - 1}{3\phi}} \right\rceil, \left\lfloor \left(\frac{\alpha}{2\,\mathrm{FW}(\square C)\phi}\right)^{2/3} \right\rceil, k_0 \right\}$;
else if $\mathrm{BBN}(\cdot) \in \mathrm{CG}(\cdot)$ **then**
  Set $K = \left\{1, \left\lfloor \left(\frac{8A - 4A^2 - 1}{6\phi}\right)^{1/3} \right\rceil, \left\lfloor \left(\frac{\alpha}{4\,\mathrm{FW}(\square C)\phi}\right)^{2/5} \right\rceil, k_0 \right\}$;
end
Remove from K all those elements k that are greater than k_0;
for $k \in K$ **do**
  Set $X^k = \mathsf{ApproxFW}(C, k)$;
end
Let X^* denote the set X^k for which $F(X^k)$ is minimal;
return X^*;

Algorithm 3: Algorithm $\mathsf{HubPlacement}(C, \phi, k_0)$ takes as input a convex polygon C, a backbone network topology $\mathrm{BBN}(\cdot)$, a positive scalar ϕ, and a positive integer k_0.

Algorithm 2 for particular input values of k, which are determined by A, ϕ, $\mathrm{FW}(\square C)$, and k_0. (For example, when $\mathrm{BBN}(\cdot) = \mathrm{MST}(\cdot)$, we would use the four values $K = \{1, \lfloor w/h \rceil, \alpha/2\phi, k_0\}$.) In the following section, we will explain why our use of these particular values of k results in a constant-factor approximation algorithm for minimizing (25).

As stated previously, this paper will deal with the special case where $\mathrm{BBN}(\cdot) = \mathrm{SN}(\cdot)$. As stated in Algorithm 3, we consider only those elements of the set

$$K = \left\{1, \left\lfloor \sqrt{\frac{24A - 12A^2 - 3}{9\phi}} \right\rceil, \left\lfloor \frac{2^{1/3}\alpha^{2/3}}{2\,\mathrm{FW}(\square C)^{2/3}\phi^{2/3}} \right\rceil, k_0 \right\}$$

that are bounded above by k_0. For purposes of brevity, we will consider the case where all elements of K are at most k_0, so that our upper and lower bounds are not affected by k_0; the general proof merely requires a case-by-case analysis on the relationships between k_0 and the other elements of K and can be solved using precisely the same kind of approach we take here. See the Online Supplement of [8] for an example of how one would do this for the special case where $\mathrm{BBN}(\cdot) = \mathrm{TSP}(\cdot)$, for example.

Upper bound I When $k = 1$, it is clear that $F(X)$ is bounded above by $\mathrm{FW}(C) \leq H(A, 1/h, h)$.

Upper bound II When $k = \left\lfloor \sqrt{\frac{8A-4A^2-1}{3\phi}} \right\rceil$, then provided that $w/k \geq h/2$, we know from Claim 23 that Algorithm 1 divides $\square C$ into k identical rectangles with dimensions $w/k \times h$ and places the points X at their centers. The backbone network cost of such a configuration is clearly

$$\sum_{i=1}^{k} |i - (k+1)/2| \cdot w/k = \begin{cases} \frac{wk}{4} & \text{if } k \text{ is even} \\ \frac{w(k^2-1)}{4k} & \text{if } k \text{ is odd} \end{cases}$$

and the Fermat-Weber cost is at most $k \cdot H(A/k, w/k, h)$ (here we have used the monotonicity and concavity properties in Remark 20). Thus, objective function (25) is at most

$$\phi \left(\sum_{i=1}^{k} |i - (k+1)/2| \cdot w/k \right) + k \cdot H(A/k, w/k, h)\,. \tag{31}$$

It turns out that when $w/k < h/2$ the case $k = \left\lfloor \sqrt{\frac{8A-4A^2-1}{3\phi}} \right\rceil$ is never optimal (we prefer upper bound III, described below).

Upper bound III When $k = \left\lfloor \left(\frac{\alpha}{2\,\mathrm{FW}(\square C)\phi}\right)^{2/3} \right\rceil$, then provided that $k \geq w/3h$, we are guaranteed (by Claim 22) that all rectangles output by Algorithm 1 have an aspect ratio not exceeding 3, and therefore $\mathrm{FW}(X, C) \leq \alpha/\sqrt{k}$ as in Claim 25. We can also show that $\mathrm{SN}(X) \leq k \cdot \mathrm{FW}(\square C)$: if we assume that $\square C$ is oriented so that its center is the origin, then letting Z denote a point selected uniformly at random in $\square C$, it is obvious that $\mathbf{E}(||Z||) = \mathrm{FW}(\square C)$ (since $\mathrm{Area}(\square C) = 1$). We can also think of Z as being generated by uniformly selecting one of the rectangles R_i output by Algorithm 1, then sampling a point Z_i uniformly within R_i. It follows that

$$\begin{aligned} k \cdot \mathrm{FW}(\square C) &= k \cdot \mathbf{E}(||Z||) \\ &= k \cdot \mathbf{E}\left(\mathbf{E}\left(\|Z_i\| \mid Z_i \in R_i\right)\right) \\ &\geq k \cdot \mathbf{E}\left(c_i\right) = k \cdot \left(\frac{1}{k}\sum_{i=1}^{k} ||c_i||\right) = \mathrm{SN}(X) \end{aligned}$$

where we have applied the law of iterated expectation and Jensen's inequality. Thus, we we find that objective function (25) is at most

$$\phi k \cdot \mathrm{FW}(\square C) + \alpha/\sqrt{k}\,.$$

By differentiating with respect to k and looking at the highest order terms we can verify that as $\phi \to 0$, the above expression approaches

$$\frac{3\alpha^{2/3}}{2^{2/3}}\,\mathrm{FW}(\Box C)^{1/3}\phi^{1/3}\,.$$

We do not use this upper bound when $k < w/3h$ because Claim 22, and therefore Claim 25, does not apply (we must use either upper bound I or II).

7 Proof of approximation bounds

We note here that the preceding upper and lower bounds for the objective function $\phi\,\mathrm{SN}(X)+\mathrm{FW}(X,C)$ depend only on the input parameters A, h, and ϕ. Thus, in order to prove that Algorithm 3 minimizes (25) within a constant factor, it will suffice to show that for any triplet $(A,h,\phi)\in[1/2,1]\times(0,1]\times(0,\infty)$, there exists an upper bound UB and a lower bound LB such that UB/LB is less than some constant factor. In our particular case we will show that UB/LB ≤ 5.86. In what follows we will decompose the domain $[1/2,1]\times(0,1]\times(0,\infty)$ into a collection of sub-domains that we will address individually. Alternatively, for fixed A, one can visualize the approximation ratio over varying h and ϕ by plotting the ratio of the minimum of upper bounds I, II, and III to the maximum of the lower bounds; see Figure 11, for example.

7.1 Case-by-case analysis of the input domain

Throughout this section we set $\epsilon_1 = 1/10$ and $\epsilon_2 = 1/4$.

- Suppose that $\phi > 1$. Then it is easy to see that upper bound I of $\mathrm{FW}(C) \leq H(A,1/h,h)$ is always within a factor of 5.5 of the lower bound of Theorem 17 with $p = 1/5$; the approximation ratio is

$$\frac{\mathrm{UB}}{\mathrm{LB}} = \frac{H(A,1/h,h)}{\frac{4\sqrt{10}A^{3/2}\sqrt{\phi}-5A\phi}{50h}} < 5.5$$

  for $A\in[1/2,1]$, $h\in(0,1)$, and $\phi>1$.

- Suppose that $(h,\phi)\in(0,\epsilon_1]\times(0,\epsilon_2]$. Consider the curves in this box of the form $\{(h,\phi):\phi = ch^4\}$ for $c \geq 0.05$. If we use upper bound II, then it is not hard to see that, as k is large (since ϕ is small), the aspect ratios of the rectangles R_i are all approximately constant along the curve. The upper bound for our objective function is then approximately

$$\phi\left(\sum_{i=1}^{k}|i-(k+1)/2|\cdot w/k\right)+k\cdot H(A/k,w/k,h)\approx\left[\frac{\sqrt{24A-12A^2-3}}{12}\sqrt{c}+\left(\frac{3}{8A-4A^2-1}\right)^{1/4}\alpha' c^{1/4}\right]h$$

  where we define

$$\alpha' = H\left(A,\left(\frac{3c}{8A-4A^2-1}\right)^{1/4},\left(\frac{8A-4A^2-1}{3c}\right)^{1/4}\right).$$

  Using the lower bound of Theorem 17 with $p = 1/3$, the approximation ratio is therefore

$$\begin{aligned}\frac{\mathrm{UB}}{\mathrm{LB}} &= \frac{\left[\frac{\sqrt{24A-12A^2-3}}{12}\sqrt{c}+\left(\frac{3}{8A-4A^2-1}\right)^{1/4}\alpha' c^{1/4}\right]h}{\frac{\sqrt{6}A^{3/2}\sqrt{\phi}}{9h}-\frac{\phi A}{6h}} = \frac{\left[\frac{\sqrt{24A-12A^2-3}}{12}\sqrt{c}+\left(\frac{3}{8A-4A^2-1}\right)^{1/4}\alpha' c^{1/4}\right]h}{\frac{\sqrt{6}A^{3/2}\sqrt{c}h}{9}-\frac{Ach^3}{6}}\\ &\approx \frac{\frac{3\sqrt{24A-12A^2-3}}{4}\sqrt{c}+9\left(\frac{3}{8A-4A^2-1}\right)^{1/4}\alpha' c^{1/4}}{\sqrt{6}A^{3/2}\sqrt{c}}\end{aligned}$$

which is bounded above by 5.5 for $c \geq 0.05$ and $A \in [1/2, 1]$. Conversely, if $c < 0.05$, then it is easy to verify that $k = \left\lfloor \frac{2^{1/3}\alpha^{2/3}}{2\,\mathrm{FW}(\square C)^{2/3}\phi^{2/3}} \right\rceil \geq w/3h$, so we can apply upper bound III. Since k is large and h and ϕ are both small, the upper bound is approximately

$$\frac{3\alpha^{2/3}}{2^{2/3}}\,\mathrm{FW}(\square C)^{1/3}\phi^{1/3} \approx \frac{3 \cdot 2^{\dot{2}/3}\alpha^{2/3}}{4} c^{1/3} h\,.$$

Using the lower bound of Theorem 15, the approximation ratio is therefore

$$\begin{aligned}\frac{\mathrm{UB}}{\mathrm{LB}} &= \frac{\frac{3 \cdot 2^{\dot{2}/3}\alpha^{2/3}}{4} c^{1/3} h}{\frac{3^{4/3}A^{4/3}}{8\pi^{1/3}} \cdot \frac{\phi^{1/3}}{h^{1/3}} - \frac{A}{8} \cdot \frac{\phi}{h}} = \frac{\frac{3 \cdot 2^{\dot{2}/3}\alpha^{2/3}}{4} c^{1/3} h}{\frac{3^{4/3}A^{4/3}}{8\pi^{1/3}} \cdot \frac{(ch^4)^{1/3}}{h^{1/3}} - \frac{A}{8} \cdot \frac{ch^4}{h}} \\ &\approx \frac{2^{5/3}3^{2/3}\pi^{1/3}\alpha^{2/3}}{3A^{4/3}} < 4\end{aligned}$$

for $A \in [1/2, 1]$.

- Suppose that $(h, \phi) \in [\epsilon_1, 1] \times (0, \epsilon_2]$. As before, the upper bound is approximately

$$\frac{3\alpha^{2/3}}{2^{2/3}}\,\mathrm{FW}(\square C)^{1/3}\phi^{1/3} \approx \frac{3 \cdot 2^{\dot{2}/3}\alpha^{2/3}}{4} c^{1/3} h$$

and the lower bound of Theorem 12 is approximately

$$\frac{6 \cdot \sqrt{7} \cdot 21^{1/3} A^{7/6}}{49\sqrt{\pi}} \cdot \phi^{1/3}$$

so that

$$\frac{\mathrm{UB}}{\mathrm{LB}} = \frac{\frac{3\alpha^{2/3}}{2^{2/3}}\,\mathrm{FW}(\square C)^{1/3}\phi^{1/3}}{\frac{6 \cdot \sqrt{7} \cdot 21^{1/3}A^{7/6}}{49\sqrt{\pi}} \cdot \phi^{1/3}} = \frac{\frac{3\alpha^{2/3}}{2^{2/3}} 49\sqrt{\pi}\,\mathrm{FW}(\square C)^{1/3}}{6 \cdot \sqrt{7} \cdot 21^{1/3} A^{7/6}} < 5$$

since $h \geq \epsilon_1$ (this allows us to bound the term $\mathrm{FW}(\square C)^{1/3}$).

- Suppose that $(h, \phi) \in (0, \epsilon_1] \times [\epsilon_2, 1])$. We can use upper bound I of $\mathrm{FW}(C) \leq H(A, 1/h, h)$ and the lower bound of Theorem 17 with $p = 1/5$ so that the approximation ratio is

$$\frac{\mathrm{UB}}{\mathrm{LB}} = \frac{H(A, 1/h, h)}{\frac{4\sqrt{10}A^{3/2}\sqrt{\phi} - 5A\phi}{50h}} \sim \frac{\frac{2}{3}A/h - \frac{1}{12h} - \frac{1}{3} \cdot \frac{A^2}{h}}{\frac{4\sqrt{10}A^{3/2}\sqrt{\phi} - 5A\phi}{50h}} = \frac{100A/3 - 50A^2/3 - 25/6}{4\sqrt{10}A^{3/2}\sqrt{\phi} - 5A\phi} \leq 5.2$$

for $\phi \geq \epsilon_2$ and $A \in [1/2, 1]$.

- The final sub-domain is $(h, \phi) \in [\epsilon_1, 1] \times [\epsilon_2, 1]$. This domain is compact and closed and therefore we can verify that the approximation ratio is bounded above by 5.86 using a computational branch-and-bound procedure (one can easily verify this for the cases $A \in \{1/2, 3/4, 1\}$, for example, by inspecting Figure 11).

7.2 Summary table

Table 4 lists the values of k that we use in Algorithm 3 for the various backbone network topologies and the resulting approximation ratios.

8 Conclusions

We have considered a continuous hub-and-spoke location problem in the plane in which our objective is to balance the fixed costs and transportation costs in providing service to a planar region R. One natural extension to the model proposed here would be to consider a *transport map* $\Gamma : R \times R \to \mathbb{R}$ such that $\Gamma(x, y)$ denotes the amount of "travel" in the region between points x and y; rather than charging a cost $\phi\,\mathrm{BBN}(X)$, we would then instead charge a cost that depended on the amount of *flow* that would occur over each edge of the backbone network, given the map $\Gamma(x, y)$. It appears that even if the map $\Gamma(\cdot)$ is constant, the resulting problem brings with it a considerable set of challenges.

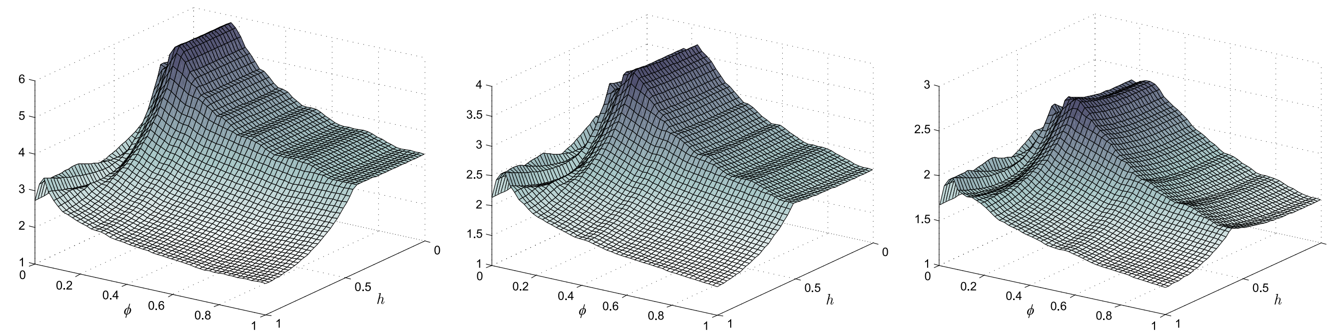

(a) $A = 1/2$ (b) $A = 3/4$ (c) $A = 1$

Figure 11: Surface plots of the approximation ratio for $h \in (0, 1]$, $\phi \in (0, 1]$, and $A \in \{1/2,\ 3/4,\ 1\}$.

Backbone network	Values of k	Approximation ratio
Steiner, MST	$1, \lfloor 1/h^2 \rceil, \lfloor {}^{\alpha}/_{\sqrt{3}\phi} \rceil$	3.12
TSP	$1, \lfloor 1/h^2 \rceil, \lfloor {}^{\alpha}/_{2\phi} \rceil$	3.70
Star network	$1, \left\lfloor \sqrt{\frac{8A-4A^2-1}{3\phi}} \right\rceil, \left\lfloor \left(\frac{\alpha}{2\,\mathrm{FW}(\square C)\phi} \right)^{2/3} \right\rceil$	5.86
Complete graph	$1, \left\lfloor \left(\frac{8A-4A^2-1}{6\phi} \right)^{1/3} \right\rceil, \left\lfloor \left(\frac{\alpha}{4\,\mathrm{FW}(\square C)\phi} \right)^{2/5} \right\rceil$	7.69

Table 4: Values of k that Algorithm 3 inputs to Algorithm 2 in order to achieve the approximation guarantees for (25) shown.

Acknowledgments

The authors thank thank the editors, two anonymous referees, Saif Benjaafar, Gérard Cachon, Robert Eberhart, David Levinson, and Yinyu Ye for many helpful discussions.

References

[1] P. Arnold, D. Peeters, and I. Thomas. Modelling a rail/road intermodal transportation system. *Transportation Research Part E: Logistics and Transportation Review*, 40(3):255 – 270, 2004.

[2] M. G. Bardossy and S. Raghavan. Dual-based local search for the connected facility location and related problems. *INFORMS Journal on Computing*, 22(4):584–602, Fall 2010.

[3] J. Beardwood, J. H. Halton, and J. M. Hammersley. The shortest path through many points. *Mathematical Proceedings of the Cambridge Philosophical Society*, 55(4):299–327, 1959.

[4] O. Berman, P. Jaillet, and D. Simchi-Levi. Location-routing problems with uncertainty. In Z. Drezner, editor, *Facility Location: A Survey of Applications and Methods*, pages 427–452. Springer, 1995.

[5] G. P. Cachon. Retail store density and the cost of greenhouse gas emissions. Working paper, 2013.

[6] J. F. Campbell. Continuous and discrete demand hub location problems. *Transportation Research Part B: Methodological*, 27(6):473 – 482, 1993.

[7] J. F. Campbell. Hub location and the p-hub median problem. *Operations Research*, 44(6):pp. 923–935, 1996.

[8] J.G. Carlsson and F. Jia. Continuous facility location with backbone network costs. *Transportation Science*, under 3rd round of review. See `http://menet.umn.edu/~jgc/minimizing-emissions-rev2.pdf`.

[9] J.G. Carlsson, F. Jia, and Y. Li. An approximation algorithm for the continuous k-medians problem in a convex polygon. *INFORMS Journal on Computing*, To appear.

[10] C. Daganzo. *Logistics Systems Analysis.* Springer, 2005.

[11] C. F. Daganzo and G. F. Newell. Configuration of physical distribution networks. *Networks*, 16(2):113–132, 1986.

[12] B. A. Davis and M. A Figliozzi. A methodology to evaluate the competitiveness of electric delivery trucks. *Transportation Research Part E: Logistics and Transportation Review*, 49(1):8–23, 2013.

[13] Z. Drezner and A. Suzuki. Covering continuous demand in the plane. *Journal of the Operational Research Society*, 61(5):878–881, 2010.

[14] J.H. Gittell. *The Southwest Airlines Way.* McGraw-Hill, 2005.

[15] S. Gordon and R. de Neufville. Design of air transportation networks. *Transportation Research*, 7(3):207 – 222, 1973.

[16] M. Haimovich and Thomas L. Magnanti. Extremum properties of hexagonal partitioning and the uniform distribution in Euclidean location. *SIAM J. Discrete Math.*, 1:50–64, 1988.

[17] M. Haimovich and A. H. G. Rinnooy Kan. Bounds and heuristics for capacitated routing problems. *Mathematics of Operations Research*, 10(4):527–542, 1985.

[18] M. P. Helme and T. L. Magnanti. Designing satellite communication networks by zero-one quadratic programming. *Networks*, 19(4):427–450, 1989.

[19] M. Hesse and J. P. Rodrigue. The transport geography of logistics and freight distribution. *Journal of Transport Geography*, 12(3):171 – 184, 2004.

[20] D. S. Hochbaum. When are NP-hard location problems easy? *Annals of Operations Research*, 1:201–214, 1984.

[21] O. Jabali, M. Gendreau, and G. Laporte. A continuous approximation model for the fleet composition problem. *Transportation Research Part B: Methodological*, 46(10):1591–1606, 2012.

[22] P. Jaillet, G. Song, and G. Yu. Airline network design and hub location problems. *Location Science*, 4(3):195–212, October 1996.

[23] M. Labbï¿œ and H. Yaman. Solving the hub location problem in a star-star network. *Networks*, 51(1):19–33, 2008.

[24] A. Langevin, P. Mbaraga, and J. F. Campbell. Continuous approximation models in freight distribution: An overview. *Transportation Research Part B: Methodological*, 30(3):163 – 188, 1996.

[25] T. L. Magnanti and R. T. Wong. Network design and transportation planning: models and algorithms. *Transportation Science*, 18(1):1–55, 1984.

[26] A. Mas-Colell, M.D. Whinston, and J.R. Green. *Microeconomic Theory*. Oxford University Press, USA, 1995.

[27] S. Melkote and M. S. Daskin. An integrated model of facility location and transportation network design. *Transportation Research Part A: Policy and Practice*, 35(6):515 – 538, 2001.

[28] P. A. Miranda and R. A. Garrido. Incorporating inventory control decisions into a strategic distribution network design model with stochastic demand. *Transportation Research Part E: Logistics and Transportation Review*, 40(3):183 – 207, 2004.

[29] G. Nagy and S. Salhi. Location-routing: Issues, models and methods. *European Journal of Operational Research*, 177(2):649 – 672, 2007.

[30] G. F. Newell. Scheduling, location, transportation, and continuum mechanics; some simple approximations to optimization problems. *SIAM Journal on Applied Mathematics*, 25(3):pp. 346–360, 1973.

[31] G. F. Newell. Design of multiple-vehicle delivery tours - III valuable goods. *Transportation Research Part B: Methodological*, 20(5):377–390, 1986.

[32] G. F. Newell and C. F. Daganzo. Design of multiple-vehicle delivery tours - I a ring-radial network. *Transportation Research Part B: Methodological*, 20(5):345–363, 1986.

[33] G. F. Newell and C. F. Daganzo. Design of multiple vehicle delivery tours - II other metrics. *Transportation Research Part B: Methodological*, 20(5):365–376, 1986.

[34] S. Nickel, A. Schobel, and T. Sonnebon. Hub location problems in urban traffic networks. In M. Pursula and J. Niittymhaki, editors, *Mathematical Methods on Optimization in Transportation Systems*, pages 95–107. Kluwer Academic Publishers, 2000.

[35] M. O'Kelly. A geographer's analysis of hub-and-spoke networks. *Journal of Transport Geography*, 6(3):171 – 186, 1998.

[36] M.E. O'Kelly and H.J. Miller. The hub network design problem: a review and synthesis. *Journal of Transport Geography*, 2(1):31–40, 1994.

[37] J. Petrek and V. Sledt. A large hierarchical network star-star topology design algorithm. *European Transactions on Telecommunications*, 12(6):511–522, 2001.

[38] M. Pinedo. *Scheduling: theory, algorithms, and systems*. Springer, 2008.

[39] L. Qi and Z. M. Shen. Worst-case analysis of demand point aggregation for the euclidean p-median problem. *European Journal of Operational Research*, 202:434–443, 2010.

[40] C. Redmond and J. E. Yukich. Limit theorems and rates of convergence for euclidean functionals. *The Annals of Applied Probability*, 4(4):pp. 1057–1073, 1994.

[41] J.P. Rodrigue, C. Comtois, and B. Slack. *The Geography of Transport Systems*. Routledge, 2009.

[42] Z.-J. M. Shen and L. Qi. Incorporating inventory and routing costs in strategic location models. *European Journal of Operational Research*, 179(2):372–389, 2007.

[43] D. Simchi-Levi, J. P. Peruvankal, N. Mulani, B. Read, and J. Ferreira. Is it time to rethink your manufacturing strategy? *MIT Sloan Management Review*, 53(2):19–22, 2012.

[44] J. M. Steele. Subadditive euclidean functionals and nonlinear growth in geometric probability. *The Annals of Probability*, 9(3):pp. 365–376, 1981.

[45] V. V. Vazirani. *Approximation Algorithms*. Springer, 2004.

[46] J. Woxenius. Conceptual modelling of an intermodal express transport system. In *International Congress on Freight Transport Automation and Multimodality Delft*, 2002.

[47] H. Yaman and S. Elloumi. Star p-hub center problem and star p-hub median problem with bounded path lengths. *Computers & Operations Research*, 39(11):2725 – 2732, 2012.

[48] D. C. Youla and H. Webb. Image restoration by the method of convex projections: Part 1: Theory. *Medical Imaging, IEEE Transactions on*, 1(2):81–94, October 1982.

[49] E. Zemel. Probabilistic analysis of geometric location problems. *Annals of Operations Research*, 1:215–238, 1984. 10.1007/BF01874390.

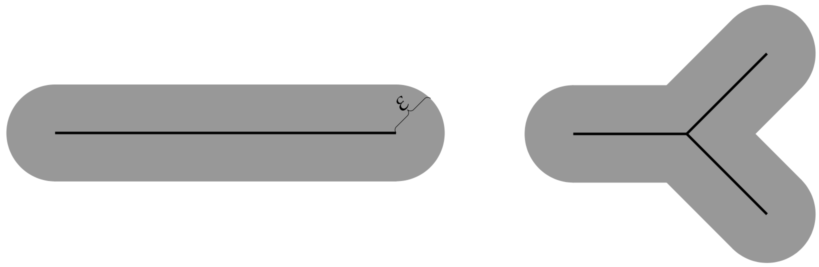

(a) (b)

Figure 12: The neighborhoods $N_\epsilon(T)$ for two trees of the same length, a line segment (12a) and a generic tree (12b).

Online supplement to "Euclidean hub-and-spoke networks"

A Proof of Lemma 3

Lemma 3 is itself a consequence of two simple claims, which we will now prove:

Claim 26. For any tree T of length ℓ and any ϵ, we have $\text{Area}\left(N_\epsilon\left(T\right)\right) \leq \pi\epsilon^2 + 2\epsilon\ell$, which is tight when T is a line segment.

Proof. We prove this by induction on the number of line segments k that comprise T. The base case $k = 1$ is simply a line segment for which $N_\epsilon\left(T\right)$ is shown in Figure 12a. To complete the induction, consider a tree consisting of k line segments, which we can think of as the union of a tree $T^{'}$ with length $\ell^{'}$ with $k-1$ line segments, and a line segment s of length $\ell^{''}$ such that $\ell = \ell^{'} + \ell^{''}$. Let $T^{'} \cup s = T$ denote their union. Since $T^{'}$ and s are joined at a point, the neighborhoods $N_\epsilon(T^{'})$ and $N_\epsilon(s)$ must both contain a ball of radius ϵ about their point of intersection; in other words, we have $\text{Area}(N_\epsilon(T^{'}) \cap N_\epsilon\left(s\right)) \geq \pi\epsilon^2$ and therefore we find that

$$\begin{aligned}\text{Area}\left(N_\epsilon\left(T\right)\right) &= \text{Area}\left(N_\epsilon\left(T^{'} \cup s\right)\right) = \text{Area}\left(N_\epsilon\left(T^{'}\right) \cup N_\epsilon\left(s\right)\right) \\ &= \underbrace{\text{Area}\left(N_\epsilon\left(T^{'}\right)\right)}_{\leq \pi\epsilon^2 + 2\epsilon\ell'} + \underbrace{\text{Area}\left(N_\epsilon\left(s\right)\right)}_{\leq \pi\epsilon^2 + 2\epsilon\ell''} - \underbrace{\text{Area}\left(N_\epsilon\left(T^{'}\right) \cap N_\epsilon\left(s\right)\right)}_{\geq \pi\epsilon^2}\end{aligned}$$

and the desired result follows. □

Claim 27. Let T denote a tree with length ℓ and let R denote a planar region with area A containing T. Further let L denote a line segment with length ℓ and let $\epsilon_L^{\max}$ be chosen so that $\text{Area}(N_{\epsilon_L^{\max}}(L)) = A$. Then $\text{FW}(L, N_{\epsilon_L^{\max}}(L)) \leq \text{FW}(T, R)$; in other words, for a given area A, among all trees with fixed length ℓ, a line segment and its appropriately-chosen neighborhood have the minimal Fermat-Weber value.

Proof. Assume without loss of generality that $A = 1$ and let $\epsilon_T^{\max}$ be chosen so that $\text{Area}(N_{\epsilon_T^{\max}}(T)) = A = 1$. It is obvious that $\text{FW}(T, N_{\epsilon_T^{\max}}(T)) \leq \text{FW}(T, R)$ for all regions R with area 1. Thus it will suffice to show that $\text{FW}(T, N_{\epsilon_T^{\max}}(T)) \geq \text{FW}(L, N_{\epsilon_L^{\max}}(L))$. Consider a random variable ϵ_T defined by setting $\epsilon_T := D\left(z, T\right)$, where z is a random variable sampled uniformly from $N_{\epsilon_T^{\max}}(T)$, and define ϵ_L similarly. Note that the cumulative distribution functions for ϵ_T and ϵ_L are given by

$$\begin{aligned}F_T(\epsilon_T) &= \min\left\{1, \text{Area}\left(N_{\epsilon_T}\left(T\right)\right)\right\} \\ F_L(\epsilon_L) &= \min\left\{1, \text{Area}\left(N_{\epsilon_L}\left(L\right)\right)\right\}\,.\end{aligned}$$

By Claim 26, for any $\epsilon > 0$, we have $F_L(\epsilon) \geq F_T(\epsilon)$. Next note that

$$\mathbf{E}(\epsilon_L) = \int_0^\infty 1 - F_L(\epsilon)\, d\epsilon \leq \int_0^\infty 1 - F_T(\epsilon)\, d\epsilon = \mathbf{E}(\epsilon_T)\,,$$

a well-known result of first-order stochastic dominance (see page 249 of [38], for instance). The proof is complete by observing that by definition, $\mathbf{E}(\epsilon_L) = \mathrm{FW}(L, N_{\epsilon_L}(L))$ and $\mathbf{E}(\epsilon_T) = \mathrm{FW}(T, N_{\epsilon_T}(T))$. $\square$

Having established the two preceding claims, we next note that for any line segment L with length ℓ and any ϵ, we can compute

$$\begin{aligned} \mathrm{Area}(N_\epsilon(L)) &= \pi\epsilon^2 + 2\epsilon\ell \\ \mathrm{FW}\left(L, N_\epsilon\left(L\right)\right) &= \frac{2\pi\epsilon^3}{3} + \epsilon^2\ell\,. \end{aligned} \tag{32}$$

Solving equation (32) in terms of $\epsilon > 0$ and substituting, we find that

$$\mathrm{FW}\left(L, N_\epsilon\left(L\right)\right) = \frac{-2\ell^3 - 3\pi\ell\,\mathrm{Area}\left(N_\epsilon\left(L\right)\right) + \left(2\ell^2 + 2\pi\,\mathrm{Area}\left(N_\epsilon\left(L\right)\right)\right)\sqrt{\ell^2 + \pi\,\mathrm{Area}\left(N_\epsilon\left(L\right)\right)}}{3\pi^2}\,.$$

We can easily show that the above quantity is bounded below by $\frac{2A^2}{8\ell+3\sqrt{\pi A}}$, where $A = \mathrm{Area}(N_\epsilon\left(L\right))$. This is equivalent to showing that

$$\frac{\left[2\left(\ell^2 + \pi A\right)^{3/2} - 3\pi A\ell - 2\ell^3\right]\left(8\ell + 3\sqrt{\pi A}\right)}{6\pi^2 A^2} \geq 1\,.$$

Defining $t := A/\ell^2$ so that $A = \ell^2 t$, the above expression is equivalent to

$$\frac{\left[(2 + 2\pi t)\sqrt{1 + \pi t} - 3\pi t - 2\right]\left(8 + 3\sqrt{\pi t}\right)}{6\pi^2 t^2} \geq 1$$

which is easily verified using single-variable calculus. Our proof of Lemma 3 is complete; if we let T be a tree contained in a region R with area A, then

$$\mathrm{FW}\left(T, C\right) \geq \mathrm{FW}\left(T, N_{\epsilon_T^{\max}}(T)\right) \geq \mathrm{FW}\left(L, N_{\epsilon_L^{\max}}(L)\right) \geq \frac{2A^2}{8\ell + 3\sqrt{\pi A}}$$

where $\mathrm{length}(T) = \mathrm{length}(L)$ and $\epsilon_T^{\max}$ and $\epsilon_L^{\max}$ are chosen so as to induce the appropriate areas.

B Proof that $\mathrm{length}((\partial B_r) \cap C) \leq 2\sqrt{\pi A p}$

Let C, B_r, A, and p be as in the proof of Theorem 12, and define $\ell = \mathrm{length}((\partial B_r) \cap C)$. As Figure 13 shows, it is clearly always the case that $\ell r/2 \leq Ap$, or equivalently that $\ell \leq 2Ap/r$. It is of course always true that $Ap \leq \pi r^2$, or equivalently that $r \geq \sqrt{Ap/\pi}$. Combining these two facts we see that

$$\ell \leq \frac{2Ap}{r} \leq \frac{2Ap}{\sqrt{Ap/\pi}} = 2\sqrt{\pi A p}$$

as desired.

C Proof of Theorem 15

Proof. As in our proof of Theorem 12, we suppose without loss of generality that $\bar{x}$ is the origin, and define B_r about the origin as before. However, we now note that, since C is contained in a "slab" of height h, it must be the case that $\mathrm{Area}(B_r \cap C) \leq \mathrm{Area}(B_r \cap \Box C) \leq 2hr$ (see Figure 14). We again consider the lower bound for $\mathrm{SN}(X)$ defined by

$$\mathrm{SNLB}_r(X) = \sum_{i=1}^{|X|} \begin{cases} 0 & \text{if } ||x_i|| \leq r \\ r & \text{otherwise} \end{cases}$$

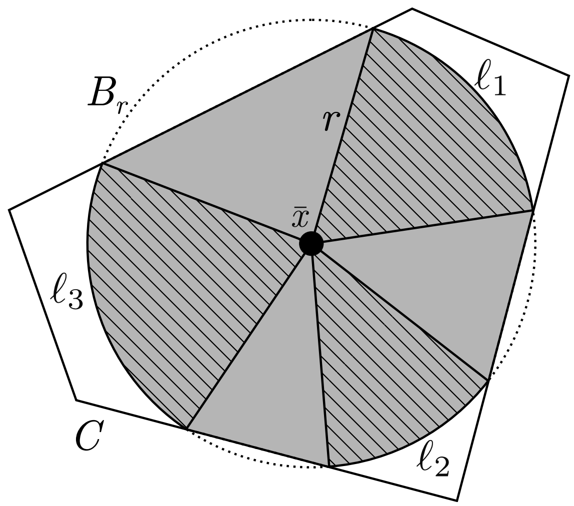

Figure 13: A convex polygon C intersecting a ball B_r. In the above diagram, we have length$((\partial B_r) \cap C) = \ell_1 + \ell_2 + \ell_3 = \ell$. The area of the hatched region, which is equal to ${}^{\ell}/_{2\pi r} \cdot \pi r^2 = \ell r/2$, is clearly a lower bound on the area $Ap = \text{Area}(C \cap B_r)$ of the shaded region.

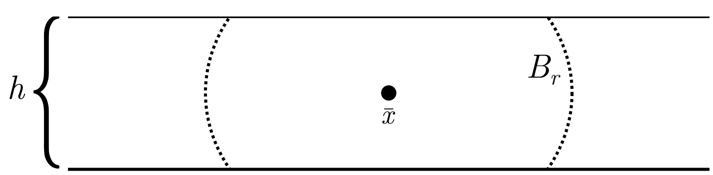

Figure 14: The setup for our proof of Theorem 15.

and look at the related problem of minimizing $\phi\,\mathrm{SNLB}_r(X) + \mathrm{FW}(X, C)$, or equivalently

$$\phi r|X \setminus B_r| + \mathrm{FW}(X, C \setminus B_r)\,.$$

We also note now that length$((\partial B_r) \cap C) \leq 4h$ (again, see Figure 14), and therefore, applying Lemma 13 with $A^{'} = A(1-p)$ and $\ell^{'} = 4h$, we find that

$$\mathrm{FW}(X, C) \geq \frac{\left(\sqrt{16h^2 + 4A(1-p)\pi(k'+1)} - 4h\right)^2 \left(2\sqrt{16h^2 + 4A(1-p)\pi(k'+1)} + 4h\right)}{24\pi^2(k'+1)^2}$$

and, using the fact that $r \geq {}^{Ap}/_{2h}$, we find that for any point set X,

$$\phi\,\mathrm{SN}(X) + \mathrm{FW}(X, C) \geq \phi k^{'} \cdot \frac{Ap}{2h} + \frac{\left(\sqrt{16h^2 + 4A(1-p)\pi(k'+1)} - 4h\right)^2 \left(2\sqrt{16h^2 + 4A(1-p)\pi(k'+1)} + 4h\right)}{24\pi^2(k'+1)^2}\,.$$

We can again remove the dependency of the right-hand side on X by taking a minimum over all $k^{'}$:

$$\phi\,\mathrm{SN}(X) + \mathrm{FW}(X, C) \geq \min_{k' \geq 0} \left\{ \phi k^{'} \cdot \frac{Ap}{2h} + \frac{\left(\sqrt{16h^2 + 4A(1-p)\pi(k'+1)} - 4h\right)^2 \left(2\sqrt{16h^2 + 4A(1-p)\pi(k'+1)} + 4h\right)}{24\pi^2(k'+1)^2} \right\}.$$

We then set $p = 1/4$ using the same reasoning as in Remark 14; plugging this value in and differentiating, we find that the optimal value of $k^{'}$ that minimizes the right-hand side of the above is

$$k^{'} = \max\left\{0\,,\ \frac{3^{1/3}A^{1/3}}{\pi^{1/3}} \cdot \frac{h^{2/3}}{\phi^{2/3}} - \frac{8 \cdot 3^{2/3}}{3\pi^{2/3}A^{1/3}} \cdot \frac{h^{4/3}}{\phi^{1/3}} - 1\right\}$$

which completes the proof. □

D Proof of Theorem 17

Proof. Assume without loss of generality that $\Box C$ is aligned with the coordinate axes and that $\bar{x}$ is the origin. Let $||\cdot||_{\leftrightarrow}$ denote the "horizontal norm", i.e. if $x = (x^1, x^2) \in \mathbb{R}^2$, then $||x||_{\leftrightarrow} = |x^1|$, and note that clearly $||x||_{\leftrightarrow} \leq ||x||$. Let B_r denote a "ball" of radius r about the origin $\bar{x}$ taken under the horizontal norm, so that B_r is simply the "slab" between two vertical lines at a distance of $2r$ apart from each other. Once again, we consider the lower bound for $\mathrm{SN}(X)$ defined by

$$\mathrm{SNLB}_r(X) = \sum_{i=1}^{|X|} \begin{cases} 0 & \text{if } ||x_i||_{\leftrightarrow} \leq r \\ r & \text{otherwise} \end{cases}$$

for some radius r, and we look at the related problem of minimizing $\phi\,\mathrm{SNLB}_r(X) + \mathrm{FW}(X, C)$, or equivalently

$$\phi r|X \setminus B_r| + \mathrm{FW}(X, C \setminus B_r)\,.$$

We also note now that length$((\partial B_r) \cap C) \leq$ length$((\partial B_r) \cap \Box C) = 2h$ so that $Ap \leq 2hr$ or equivalently $r \geq {}^{Ap}/_{2h}$, where p denotes the fraction of area of C that is contained in B_r. Following the same line of reasoning as in the proof of Lemma 13, it is easy to see that

$$\mathrm{FW}(X, C \setminus B_r) \geq \frac{A^2(1-p)^2}{4h(k'+1)}$$

where $k^{'} = |X \setminus B_r|$. This is because, if we take the Fermat-Weber value of the points X under the horizontal norm (and we assume as before that B_r contains infinitely many points from X), then we again see that the Fermat-Weber value $\mathrm{FW}(X, R)$ is minimal – over all possible regions R having area $A^{'} = A(1-p)$ – when R consists of $k^{'}$ horizontal "balls"

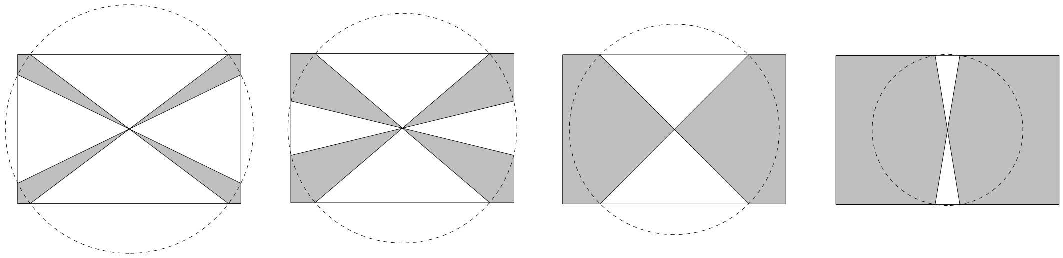

Figure 15: The worst-case regions C^* in a given box B, for increasing values of A.

of radius ϵ (i.e. horizontal slabs of width 2ϵ) plus a neighborhood of radius ϵ about B_r (i.e. a horizontal slab of width $2(r+\epsilon)$), where ϵ is chosen such that these $k^{'}$ balls and the neighborhood have area $A^{'}$, i.e. $\epsilon = A(1-p)/2h(k^{'}+1)$. The Fermat-Weber value of such a region R, under the horizontal norm, is precisely

$$(k^{'}+1)\epsilon^2 h = \frac{A^2(1-p)^2}{4h(k'+1)}$$

as desired.

We now consider the problem of choosing $k^{'}$ to minimize the sum of these lower bounds, i.e.

$$\phi\,\mathrm{SNLB}_r(X) + \mathrm{FW}(X,C) \geq \phi k^{'} \cdot \frac{Ap}{2h} + \frac{A^2(1-p)^2}{4h(k'+1)}\,,$$

which completes the proof because the above expression is minimized precisely at

$$k^{'} = \max\left\{\frac{\sqrt{A}(1-p)}{\sqrt{2p\phi}} - 1\,,\,0\right\}.$$

□

E Proof of Theorem 19

Definition 28. A region C is said to be *star convex at the point* p if the line segment from p to any point $x \in C$ is itself contained in C. Similarly, the *star convex hull* of a region S at the point p is the smallest star-convex region at the point p that contains S (i.e. the union of all segments between points $x \in S$ and p).

Lemma 29. *Let B be a box of dimensions $w \times h$ centered at the origin. The region C^* that solves the infinite-dimensional optimization problem*

$$\begin{aligned} \operatorname*{minimize}_{C}\,\mathrm{FW}\,(C) \quad & \quad s.t. \\ C \quad & \subseteq \quad B \\ \mathrm{Area}\,(C) \quad & = \quad A \\ C \quad & \ni \quad (0,0) \\ C \quad & \text{is} \quad \text{star convex at } (0,0) \end{aligned} \tag{33}$$

is the star convex hull of $B \backslash D$, where D is an appropriately chosen disk centered at the origin, as indicated in Figure 15. Furthermore for fixed w and h, the function $\Phi(A) = \mathrm{FW}(C^*)$ (i.e. the maximal value of (33)) is monotonically increasing and concave.

Proof sketch. This follows from a standard argument where we consider the integer (or linear) program obtained by discretizing problem (33) using polar coordinates. See Figure 16. Concavity of $\Phi(A)$ follows by observing that we build our optimal solution by adding sectors containing points that are strictly closer than the points in the sector that preceded them. □

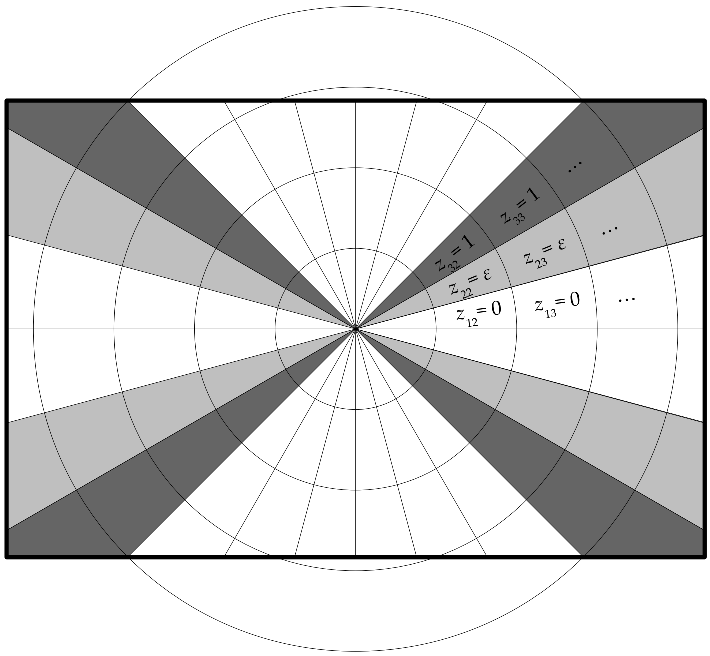

Figure 16: In the discretization above, our variables are set up in such a way that the star convexity constraint is equivalent to setting $z_{i(j+1)} \leq z_{ij}$ for all j. Since we are finding an upper bound of the Fermat-Weber value of a star-convex object in the given box, our objective is to maximize $\sum_{i,j} d_{ij} z_{ij}$ subject to the constraints that $\sum_{i,j} a_{ij} z_{ij} = A$, $z_{i(j+1)} \leq z_{ij}\ \forall i, j$, and $z_{ij} \geq 0\ \forall i, j$, where d_{ij} denotes the distance from the origin to cell ij and a_{ij} denotes the area of cell ij. By the nature of the constraints it is clear that we may assume that $z^*_{i(j+1)} = z^*_{ij}$ at optimality since the distance from cell ij to the origin increases with j. The diagram above suggests a linear programming formulation, where the lighter regions indicate fractional solutions.

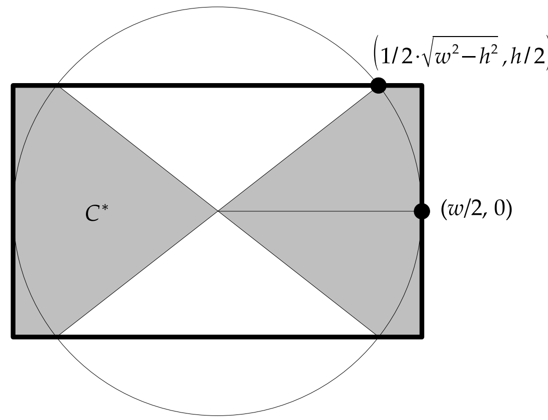

Figure 17: The area of the shaded region is $wh - \frac{h}{2}\sqrt{w^2 - h^2}$.

In order to obtain an upper bound on the output of Algorithm 2, we consider the infinite-dimensional optimization problem of choosing the worst-case convex region C that solves the problem

$$\begin{array}{rcl} \underset{C}{\text{minimize}}\, \mathrm{FW}(C) & & s.t. \\ C & \subseteq & B \\ \mathrm{Area}(C) & = & A \\ C & \ni & (0,0) \\ C & \text{is} & \text{convex.} \end{array}$$

By relaxing the convexity constraint with star convexity about the origin, the problem becomes equivalent to problem (33); we can use it to determine an upper bound on $\mathrm{FW}(C)$.

Following Lemma 29 we see that the worst-case star-convex region C^* takes the form shown in Figure 15. If $A \geq wh - \frac{h}{2}\sqrt{w^2 - h^2}$, then the optimal solution consists of two components (rather than 4) as shown in Figure 17. The bound given in Theorem 19 is precisely the Fermat-Weber value $\iint_{C^*} ||x||\, dA$ obtained by analytic integration. We can prove Remark 20 by taking the Fermat-Weber values of C^* under the ℓ_1 and ℓ_∞ norms instead (which have a much simpler closed form) and observing that

$$\iint_{C^*} ||x||_1\, dA \sim \frac{2}{3}Aw - \frac{1}{12}w^2h - \frac{1}{3} \cdot \frac{A^2}{h}$$

and

$$\iint_{C^*} ||x||_\infty\, dA \sim \frac{2}{3}Aw - \frac{1}{12}w^2h - \frac{1}{3} \cdot \frac{A^2}{h}$$

from which (30) holds by the squeeze theorem.

F Proof of Claim 22

To prove Claim 22 it is sufficient to show that the following lemma holds:

Lemma 30. *Suppose that $\tilde{R} \subseteq \square C$ is an intermediate rectangle obtained throughout Algorithm 1, which is further subdivided into $\tilde{R}^{'}$ and $\tilde{R}^{''}$; if $\mathrm{AR}(\tilde{R}) \leq 3$, then $\mathrm{AR}(\tilde{R}^{'}) \leq 3$ and $\mathrm{AR}(\tilde{R}^{''}) \leq 3$.*

Proof. Assume that $\mathrm{AR}(\tilde{R}) \leq 3$ and assume without loss of generality that $\mathrm{width}(\tilde{R}) \geq \mathrm{height}(\tilde{R})$, so that $\mathrm{height}(\tilde{R}^{'}) = \mathrm{height}(\tilde{R})$. Since $\tilde{R}$ is always divided into proportions as close as $1/2$ as possible, we have

$$\mathrm{width}(\tilde{R})/3 \leq \mathrm{width}(\tilde{R}^{'}) \leq 2\,\mathrm{width}(\tilde{R})/3$$

and, dividing by $\mathrm{height}(\tilde{R})$, we find that

$$\frac{\mathrm{width}(\tilde{R})}{3\,\mathrm{height}(\tilde{R})} \leq \frac{\mathrm{width}(\tilde{R}^{'})}{\mathrm{height}(\tilde{R}^{'})} = \frac{\mathrm{width}(\tilde{R}^{'})}{\mathrm{height}(\tilde{R})} \leq \frac{2\,\mathrm{width}(\tilde{R})}{3\,\mathrm{height}(\tilde{R})} \leq 2$$

so that $\mathrm{width}(\tilde{R}^{'})/\,\mathrm{height}(\tilde{R}^{'}) \leq 2$. Taking the reciprocal of this expression and observing that $3 \geq 3\,\mathrm{height}(\tilde{R})/\,\mathrm{width}(\tilde{R})$ since $\mathrm{width}(\tilde{R}) \geq \mathrm{height}(\tilde{R})$, we have

$$3 \geq \frac{3\,\mathrm{height}(\tilde{R})}{\mathrm{width}(\tilde{R})} \geq \frac{\mathrm{height}(\tilde{R}^{'})}{\mathrm{width}(\tilde{R}^{'})} = \frac{\mathrm{height}(\tilde{R})}{\mathrm{width}(\tilde{R}^{'})} \geq \frac{3\,\mathrm{height}(\tilde{R})}{2\,\mathrm{width}(\tilde{R})}$$

so that $3 \geq \mathrm{height}(\tilde{R}^{'})/\,\mathrm{width}(\tilde{R}^{'})$. This same argument clearly applies to $\tilde{R}^{''}$ as well, which completes the proof. $\square$